Injectable pH-responsive Ureido-Pyrimidinone (UPy) hydrogel as drug carrier for epicardial activation

MSc Thesis
Francesca Cecilia Lauta

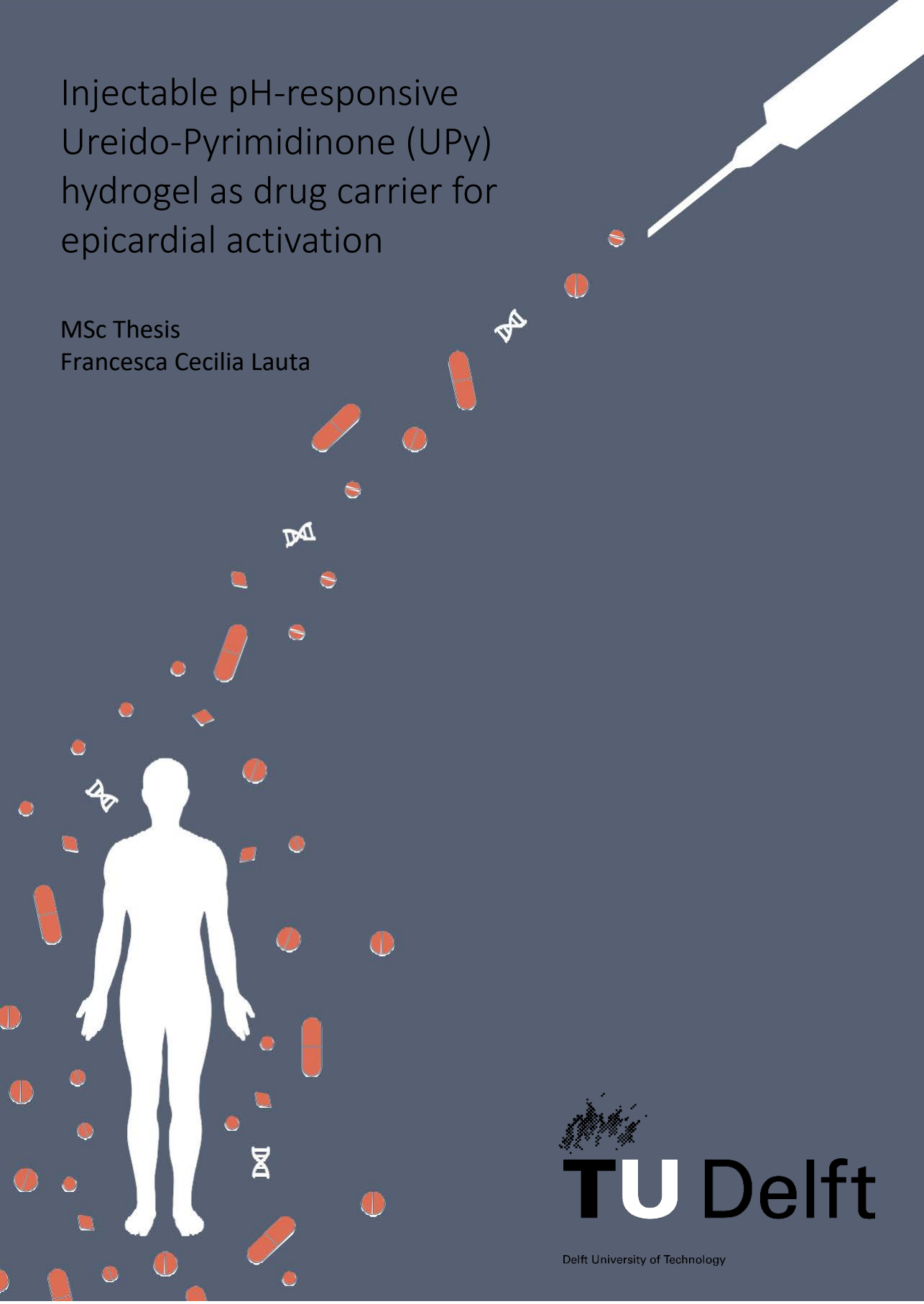

TU Delft
Delft University of Technology

Injectable pH-responsive Ureido-Pyrimidinone (UPy) hydrogel as drug carrier for epicardial activation

By

Francesca Cecilia Lauta

in partial fulfilment of the requirements for the degree of

Master of Science
in Biomedical Engineering
Biomaterials and Tissue Biomechanics specialisation track

at the Delft University of Technology
to be defended publicly on Monday April 29th, 2019 at 4:00 PM

Student number:	4625900
Supervisor TU Delft:	Dr. Ir. Lidy Fratila-Apachitei
	Prof. Dr. Ir. A. Zadpoor
Supervisors LUMC:	Prof. Marie-José Goumans
	Dr. Anke Smits
	Esther Dronkers

TU Delft Delft University of Technology

LUMC Leiden University Medical Center

To my Ithaka

Thanks for giving me
the marvellous journey

Abstract

The presence of a stem cell source in the epicardium that can be stimulated by exogenous delivery of transforming growth factor-β (TGF-β) and migrate towards the myocardium can represent a new approach to achieve cardiac repair following myocardial infarction. However, injection of drugs always requires use of carriers which help stabilize the compound in the harsh and dynamic environment of the heart. To this extent, pH-responsive drug delivery systems represent an enthralling approach to ensure minimal invasiveness, instantaneous responsiveness, and targeted delivery of the incorporated compound. In this *in vitro* study we aimed to validate an Ureidopyrimidinone-based supramolecular hydrogel as TGF-β carrier for epicardial activation. The results demonstrated the capacity of the hydrogel to respond to pH changes and deliver the growth factor, which retained its ability to activate its signalling pathway and stimulate treated cells.

Contents

List of Abbreviations

BSA: Bovine serum albumin
CFB: Cardiac fibroblast
CM: Cardiomyocyte
CVD: Cardiovascular disease
DDS: Drug delivery system
DMEM: Dulbecco modified eagle medium
DMSO: Dimethyl sulfoxide
E-Cad: Epithelial cadherin
EC: Endothelial cell
ECM: Extracellular matrix
EMT: Epithelial-to-mesenchymal transition
EPDC: Epicardial derived cell
FBS: Fetal bovine serum
MET: Mesenchymal-to-epithelial transition
MI: Myocardial infarction
N-Cad: Neural cadherin
PBS: Phosphate buffered saline
PEG: Polyethylene glycol
P/S: Penicillin and streptomycin
qPCR: quantitative polymerase chain reaction
SB: SB431542
SDS: Sodium dodecyl sulphate
SMA: Smooth muscle actin
SMC: Smooth muscle cell
TGF-β: Transforming growth factor-β
TGFβR-II: TGF-β receptor type II
UPy: Ureido-pyrimidinone
UPy-PEG: Ureido-pyrimidinone end-modified polyethylene glycol
UPy-TGFβ: UPy-PEG hydrogel with added TGF-β

1 Introduction

Cardiovascular disease (CVD) represents the leading cause of mortality in the European Union (EU), accounting for over 1.8 million deaths every year and costing €210 billion to the EU economy [1]. Amongst all CVDs, myocardial infarction (MI) constitutes the primary cause of death [1]. Most frequently, MI results from the rupture of an atherosclerotic plaque in a coronary vessel, which initiates a coagulation cascade, leading to thrombus formation [2]. Presence of a blood clot causes blockage of the artery and prevents oxygen and nutrients to reach the downstream areas, causing cells apoptosis due to hypoxia. The following state of inflammation initiates an immune response which promotes wound healing and ends with the formation of a stiff scar. Whilst providing support to the injured tissue, the scar lacks contractile properties, resulting in an abnormal cardiac output. The endocrine and nervous systems react by initiating several compensatory mechanisms aimed at improving the blood flow into the body [3]. However, the high demand placed on heart leads to hypertrophy of the viable segments, left ventricle dilatation, dysfunction and – ultimately – heart failure (Figure 1). Current surgical and pharmacological approaches aim at improving blood supply to the damaged area and decreasing the demand on the cardiac muscle by lowering the blood pressure, to slow down the development of heart failure and reduce mortality [4]. However, despite diminishing the number of deaths for acute MI, none of these therapies have been able to thwart the impaired cardiac function deriving from cardiomyocytes loss. In the most serious cases, heart transplantation remains the only option for ischemic patients, a solution strongly limited by a lack of donors and by poor long-term performance of the transplanted graft [5].

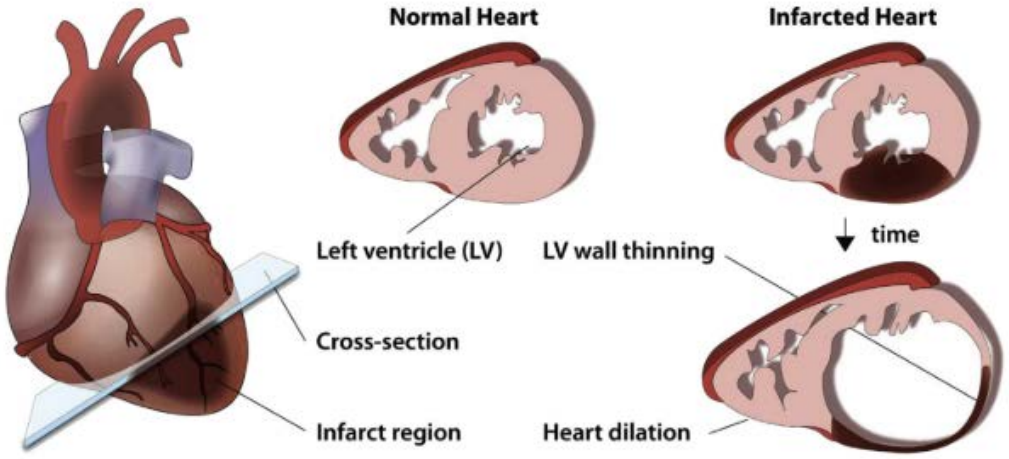

Figure 1 Heart remodeling following myocardial infarction (MI). The heart compensatory mechanisms aimed at satisfying the body's blood demand lead to thinning and dilatation of the left ventricle walls, dysfunction and progressive heart failure. Image from [6].

One of the main problems associated with MI consists of the reduced pumping capacity that derives from the massive loss of cardiomyocytes (CMs) in the infarcted area. Their yearly turn-over is only minimal and not sufficient to restore the initial population [7], thus research has worked towards the identification of progenitor cell sources able to generate new cardiac tissue [8]. Tracing experiments addressed the epicardium as a possible reservoir of stem cells, due to its major contribution in myocardial growth during embryonic development [9]–[11]. Epicardial cells derive from a cluster-like structure composed of mesenchymal and epithelial cells, known as proepicardium. During heart formation, proepicardial epithelial cells lose their epithelial phenotype and acquire mesenchymal characteristics, in a process known as epithelial-to-mesenchymal transition (EMT). They detach from the proepicardium and migrate onto the myocardial surface, where they adhere, proliferate, and undergo mesenchymal-to-epithelial transition (MET), resulting in the formation of the epicardium.

While this layer remains intact, some of its cells, the epicardial derived cells (EPDCs), go through EMT for a second time and migrate towards the myocardium, where they differentiate into vascular smooth muscle cells (SMCs) and cardiac fibroblasts (CFBs), contributing to myocardial growth and coronary vessels formation [10][12]. This process has a key role in myocardial development; indeed, errors or inhibition of EPDCs movement have been proved to be responsible of congenital heart disease, impaired growth of the coronary vasculature and the cardiac conduction system [11].

When embryonic development ends, the epicardium enters a quiescent phase [13]. However, previous studies have shown that, following myocardial injury, it can reactivate its embryonic characteristics and stimulate production and movement of EPDCs, which differentiate into SMCs and CFBs [13][14]. Despite their contribution to the CMs and endothelial cells (ECs) population has not been proved, the interest in this progenitor stem cell source remains due to the paracrine signals it secretes following MI, which have been demonstrated to promote angiogenesis, reduce infarct size and improve general heart function [13]. Interestingly, EMT can be stimulated *in vitro* through administration of transforming growth factor-β (TGF-β) [15][16]. Briefly, TGF-β binds and activates its receptor TGF-β type II (TGFβR-II), which in turn phosphorylate and activates the transcription factors Smad2/3. Smad2/3 then bind to Smad4 and translocate into the nucleus, where they regulate the expression of TGF-β-responsive genes (Figure 2) [17]–[19]. In epithelial cells administration of TGF-β is related with increased expression of N-cadherin (N-cad), smooth muscle actin (SMA), SNAI1 (Snail) and SNAI2 (Slug) and in the downregulation of epithelial cadherin (E-cad) [20]–[24].

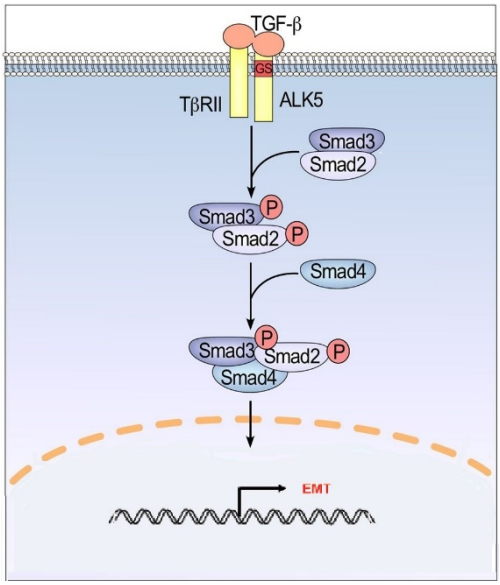

Figure 2 TGF-β/SMAD signalling pathway. When TGF-β binds to its receptor, it triggers Smad2/3 phosphorylation. Smad2/3 then form a trimeric complex with Smad4, which enters the nucleus and modulates expression of EMT-related genes. Image adapted from [25].

The role of TGF-β during induced EMT suggests that exogenous delivery of this growth factor may trigger epicardial activation and EPDCs movement, representing a new approach to achieve cardiovascular repair. However, *in vivo* injection of secretory factors didn't confirm to be an effective strategy mostly due to the compounds' instability in the harsh and contracting environment of the heart. Increasing the concentration mostly lead to harmful side effects [26]–[29], raising awareness for the importance of carriers in the design of new approaches for protein therapies. Drug delivery systems (DDSs) are vehicles meant to encapsulate molecules and support them when applied *in situ,* as well as provide them protection against *in vivo* degradation. They are composed of cytocompatible and biodegradable materials arranged in porous structures to allow sustained release throughout the time of application, after which their degradation products are expelled through metabolic pathways.

Some DDSs are synthetized to change their morphology in response to external stimuli, allowing for non-invasive administration to achieve minimal discomfort for the patient and reduce complications risk of surgery. Most of the times DDSs are hydrogel materials, three-dimensional crosslinked networks of polymer chains mainly composed of water. With their stiffness, they offer structural support to the damaged tissues and, at the same time, their high-water content allows them to best mimic the natural extracellular matrix (ECM), creating a favourable environment for cells and proteins activity [30][31].

In this context, hydrogels based on polyethylene-glycol (PEG) have been proposed as effective DDSs owing to their potential of encapsulating single or multiple growth factors and slowing down their degradation rate in drug-based therapies [32]–[34]. When coupled with supramolecular constructs, PEG hydrogels form highly directional and reversible non-covalent cross-links, able to network in aqueous solutions and form a transient fibrous structure in response to external stimuli [35]. So far, external triggers have been of biological, chemical and physical nature (reviewed in [36]), creating a huge pool of DDSs which can be used for controlled and targeted biomedical applications. Amongst them, pH-responsive DDSs constitute a very appealing technology, since their transition is swift, reversible and naturally takes place *in vivo,* preventing the risk of gelation during injection.

PEG polymers based on supramolecular Ureido-pyrimidinone (UPy) moieties represent a novel class of hydrogels suitable for minimally invasive drug delivery therapies, due to the presence of UPy groups which form transient hydrogen bonds with the PEG chains that can be reverted by changing the pH of the aqueous solution in which the gel is formed [34][37][38]. At basic pH, UPy-PEG gel behaves as a viscous liquid, which can be easily injected and that quickly solidifies when in contact to the body neutral pH.

1.1 Research questions

This research project aimed at demonstrating the efficacy of UPy-PEG hydrogel as TGF-β carrier for epicardial EMT stimulation. To do so, we loaded UPy-PEG with TGF-β and looked at the gel releasing capacity through different qualitative and quantitative assays. Experiments have been designed:

1) To elucidate the effectiveness of UPy-PEG as drug delivery system;
2) To verify the reproducibility of the release and understand its characteristics;
3) To confirm the activity of TGF-β following delivery.

UPy-PEG delivery capacity and the characteristics of the release have been probed through the enzyme-linked immunosorbent assay (ELISA) and the luciferase assay. Conditioned medium from releasing experiments was first analysed through ELISA, through which we quantified the amount of TGF-β released in different experiments, verified the reproducibility of the procedure as well as the gel's efficiency as a drug carrier. Analysis of these data also provided information about the kinetics of the release. The same conditioned medium was assayed through luciferase assay, with which we obtained the first proof of principle of TGF-β retained activity following delivery.

Activity of TGF-β has been probed at protein level and mRNA level on epithelial cells; these cells, compared to epicardial cells, do not present patient variation and availability problems, being easier to culture but still allowing to measure SMAD2 phosphorylation and TGF-β induced EMT. At protein level, we looked at phosphorylation of SMAD2 after stimulation of epithelial cells with UPy-TGFβ conditioned medium. Presence of SMAD2 phosphorylation indicated activation of the TGF-β signalling pathway, confirming protein functionality following release and excluding any possible interference of the gel in the compound's activity. Finally, evaluation of the genes expressed in UPy-TGFβ stimulated cells would address the question on whether UPy-PEG can be considered as an effective

DDS for cell activation. Upregulation of the mesenchymal phenotype not only confirmed the gel delivery capacity but also proved its ability to activate epithelial cells and stimulate them to undergo EMT.

2 Materials and Methods

2.1 Cell culture

Human fibrosarcoma cells (HT1080), transfected with $(CAGA)_9$ MLP-luc using FuGENE [39], were used as reporter cells for luciferase assay (Figure 3a). Human lung cancer cells (A549) were used as an epithelial cell line in Western Blot assay and quantitative polymerase chain reaction (qPCR) (Figure 3b). Both cell lines were cultured in Dulbecco's Modified Eagle Medium (DMEM, Gibco), supplemented with 10% fetal bovine serum (FBS, BioWest) and 1% penicillin/streptomycin (P/S, Roth), in T75 flasks (CellStar®) at 37°C and 5% CO_2 and passed at 70%-80% confluency every 2-3 days.

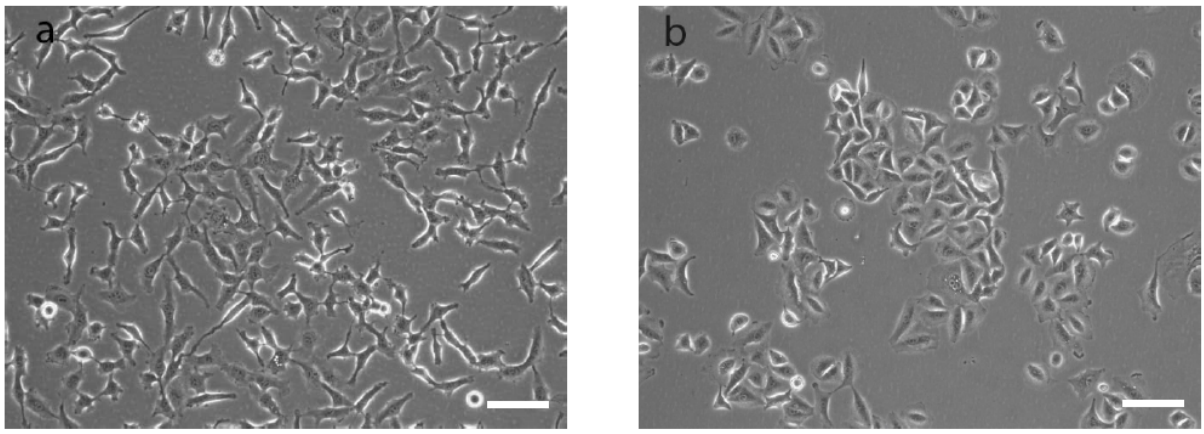

Figure 3 (a) Human fibrosarcoma CAGA-responsive cells (HT1080) used ad reporter cell line in luciferase assay. (b) Human lung cancer cells (A549), used as epithelial cell line. Scale bar = 100 µm

2.2 Drug preparation

Purified recombinant human transforming growth factor-β 3 (TGFβ-3; R&D Systems, Cat. No.: 243-B3) was reconstituted at 5ng/µL concentration in sterile Reconstitution Buffer and stored at 4°C. Reconstitution Buffer was prepared by dissolving 4 mM HCl in a solution of 0.1% bovine serum albumin (BSA, Sigma, Cat. No.: 05479) in phosphate buffered saline (PBS).
SB431542 (SB; Tocris, Cat. No.: 1614) was purchased as crystalline solid and dissolved in sterile dimethyl sulfoxide (DMSO, SeccoSolv®) at 50mM concentration and stored at -22°C. In cells experiments it was used as negative control, since it represents a potent TGF-β inhibitor [40]–[42].

2.3 TGF-β solubility

Due to its high hydrophobic nature, TGF-β strongly attaches to optical plastic surfaces where it is commonly used [43]. Therefore, different media and surfaces were tested in one preliminary experiment to determine the optimal experimental conditions.

TGF-β was dissolved at 5ng/mL as detailed in the following table (Table 1) and incubated for 24 hours at 37°C in 5% CO_2. After this time, medium was collected and added to HT1080 cells, which were assayed with luciferase after 6 hours incubation at 37°C in 5% CO_2.

SAMPLE NAME	*SOLUTION MEDIUM*	*TEST MATERIAL*
DMEM_P	serum-free DMEM supplemented with 1% Pen/Strep	24-well polystyrene plate (Corning® Costar®)
DMEM_G	serum-free DMEM supplemented with 1% Pen/Strep	Glass Petri dish
HCl/BSA/PBS	4mM HCl in 0.1% BSA/PBS	24-well polystyrene plate (Corning® Costar®)
BSA/DMEM	10 mg/mL BSA in serum-free DMEM	24-well polystyrene plate (Corning® Costar®)

Table 1 Test solutions and materials for TGF-β surface binding assessment.

2.4 UPy-PEG hydrogel formulation and release

UPy-PEG-10k (where 10k is the PEG average molecular weight measured in kg mol^{-1}) was a gift from the laboratory of Patricia Dankers (Department of Biomedical Engineering, Eindhoven University of Technology).

UPy-PEG hydrogel was prepared according to the protocol previously described by Pape et al. [37]. Briefly, basic PBS was prepared by adding aliquots of sodium hydroxide (NaOH) until the solution reached a pH of 11.7, measured under constant stirring with a pH-meter (VWR Advanced Instruments). UPy-hydrogelator – which came in powder form – was added to basic PBS to get a 10%wt solution, which was stirred at 70°C and 550 rpm for 1 hour (Figure 4a). Formation was complete when the gel looked like a homogenous and transparent liquid solution (Figure 4b), which was then cooled to 50°C for compounds addition. 50°C was set as working temperature because it prevented fast UPy-PEG increase in viscosity as well as drugs degradation.

The volume of TGF-β added to UPy-PEG hydrogel was calculated so that the conditioned medium had a concentration of 25ng/mL when all TGF-β would have been delivered. This volume of TGF-β was added to UPy-PEG hydrogel to form a 10%wt solution, named UPy-TGFβ, that was stirred at 50°C and 550rpm for 10 minutes. Well inserts (6.5mm diameter, 8.0 µm Pore Polycarbonate Membrane, Transwell®, Corning) were prepared by covering their bottom with Parafilm to prevent leakage during neutralization (Figure 5) and added to a 24-well plate. A volume of 100µL of the viscous hydrogel solution containing TGF-β was pipetted into each insert, followed by addition of 1.4µL HCl-1M which allowed solidification through pH neutralization. Gels were cured for 1 hour at room temperature.

For releasing experiments, parafilm was removed and wells were filled with releasing medium, which consisted of 10mg/mL BSA dissolved in serum-free DMEM (Figure 6). The 24-well plate was sealed with Parafilm to prevent evaporation and incubated at 37°C in 5% CO_2. Conditioned medium was removed at specific time points (3h, day 1, day 2, day 3 … day 21) and replaced with fresh one. Conditioned medium was stored in Eppendorf tubes at -22°C until use.

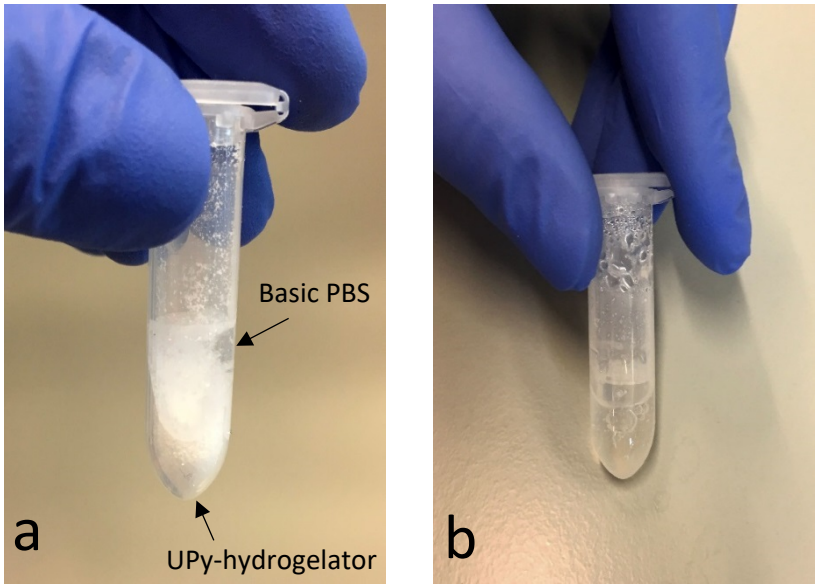

Figure 4 UPy-PEG hydrogel before and after formation. (a) UPy-PEG hydrogel before formation. The UPy hydrogelator is still a powder physically separated from the PBS. (b) After constant stirring at 70°C, the two components are mixed and result in a homogeneous liquid solution, with low viscosity.

Figure 5 Transwell inserts covered with parafilm to prevent UPy-PEG leakage during neutralization.

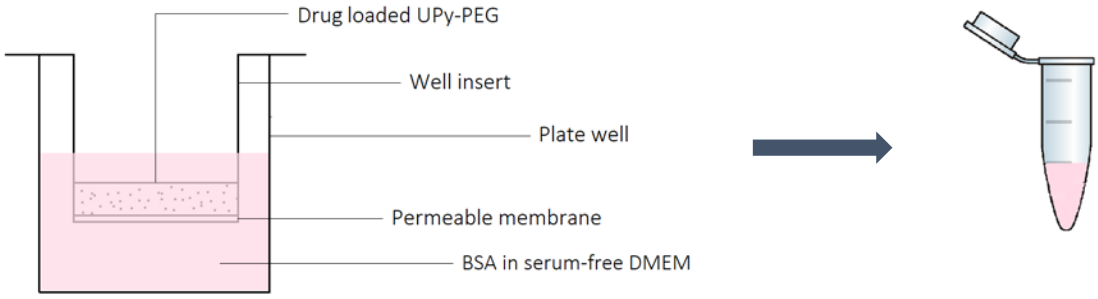

Figure 6 Schematic representation of the experimental layout for releasing experiments. Inserts filled with UPy-PEG loaded with TGF-β were placed into plate wells filled with releasing medium (10mg/mL BSA in serum-free DMEM) for releasing experiments. Conditioned medium was removed at specific time points and then stored in Eppendorf tubes.

2.5 Experimental setup

Experiments were performed using conditioned medium and control medium. Conditioned medium came from releasing experiments and was collected as explained in Section 2.4. Control medium was formed by adding TGF-β (positive control), SB and TGF-β (negative control) or no compound (simple control) to 10mg/mL BSA in serum-free DMEM. In assays where cells were used, reporter and epithelial cells were cultured with conditioned medium or control medium and then assayed. The conditions were labelled as "test sample" and "control sample" respectively (Figure 7).

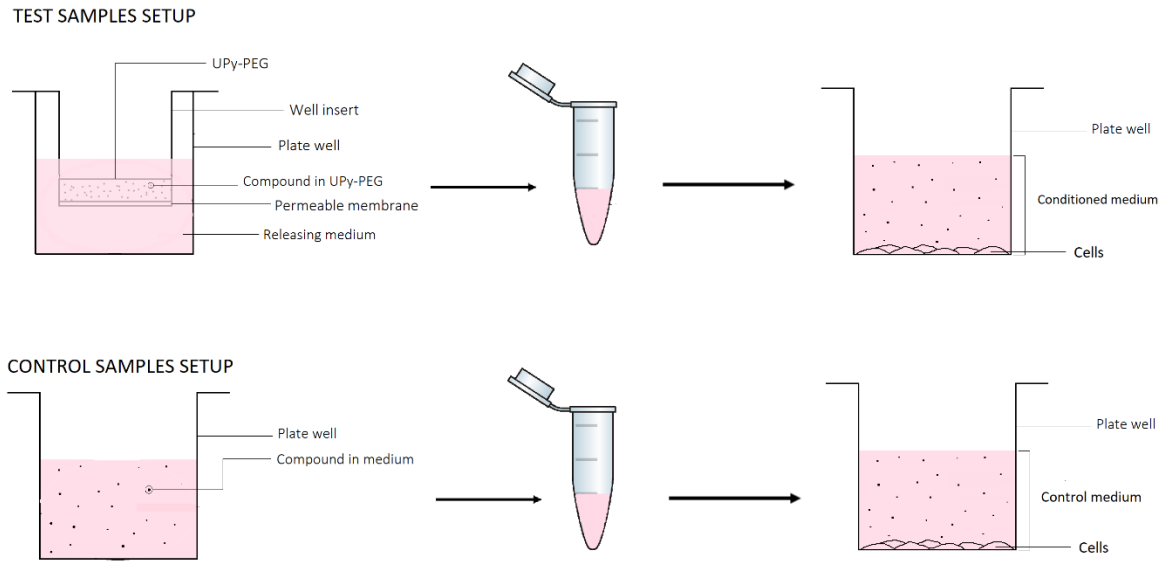

Figure 7 Experimental setup for cells experiments. Conditioned medium and control medium were stored in Eppendorf tubes. Cells were then cultured with these media and assayed.

2.6 UPy-PEG releasing capacity

UPy-PEG releasing capacity was probed quantitatively and qualitatively through enzyme-linked immunosorbent assay (ELISA) and luciferase assay, respectively. Both assays have been performed on the same conditioned media and control media in three different independent experiments, which were labelled as P1, P2 and P3.

Analysis of conditioned media with ELISA allowed us to measure the quantity of TGF-β released in different experiments, to evaluate the reproducibility of the release as well as the delivery mechanism. On the other hand, luciferase experiments with reporter cells cultured with the same conditioned media allowed to determine TGF-β retained ability to induce a cell response following delivery.

2.6.1 Quantification of UPy-TGFβ release

To quantify the amount of TGF-β released over time, we performed sandwich ELISA on conditioned media and control media coming from three independent releasing experiments, named P1, P2, P3 (Figure 8). From the Eppendorf tube where they were stored, we isolated 100µL of media that we analysed using the human TGFβ-3 DuoSet® ELISA kit (R&D systems). Test samples analysed came from UPy-TGFβ release of 3 hours, 1 day, 2 days, 3 days, 7 days, 14 days and 21 days from the beginning of the experiment. Each sample contained releasing products of one day. Analysis of these samples was performed in duplicate. The amount of active TGFβ-3 was assessed by measuring the absorbance at

450nm wavelength through a microplate reader (Synergy™ HT, BioTek®). To take into account optical imperfections in the plate, measurements were then corrected by readings at 570nm. A standard curve, which correlated mean absorbances to known sample concentrations, allowed to obtain quantities of TGFβ-3 in each sample by simple interpolation of their measured absorbance.

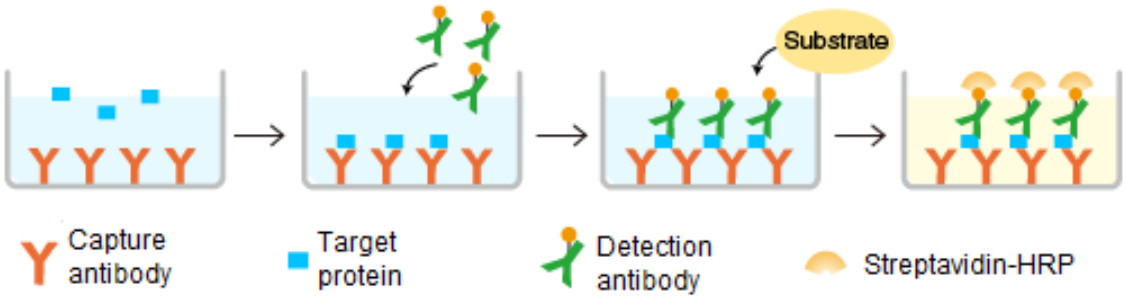

Figure 8 Schematic representation of a sandwich ELISA. The Capture Antibody is attached to the bottom surface of the plate and captures the protein of interest. The Detection antibody binds to the targeted protein and it is then visualized through the enzyme-conjugated secondary antibody horseradish peroxidase (HRP), finally turned into a fluorescent dye by application of a Substrate Solution. Image adapted from: https://www.mblintl.com/products/enzymelinked-immunosorbent-mbli/

2.6.2 Determination of the release mechanism

2.6.2.1 Korsmeyer-Peppas model

To determine the mechanism through which TGF-β was released, data coming from three independent ELISA experiments (P1, P2 and P3) were analysed through the semi-empirical Korsmeyer–Peppas model, which constitutes the preferred method to study release from polymeric systems like hydrogels [44]. According to this model, drug release has an exponential relationship with time and it can be described by the following equation:

$$F = \frac{M_t}{M_\infty} = K \cdot t^n \tag{1}$$

where F is the amount of drug released, M_t is the amount of compound released at time t, M_∞ is the amount of drug in the system, K is the kinetic constant which characterises the UPy-TGFβ system and n the exponent of release in function of time t. Analysis has been done through a non-linear fitting method to which we applied perfect sink boundary conditions, that is:

1) One-dimensional release through a thin polymer slab;
2) Uniform TGF-β concentration into the system at t = 0;
3) Constant TGF-β diffusivity through UPy-PEG.

Depending on the value of the exponent n, release can be defined as Fickian or Non-Fickian (Table 2). To determine the exponent n, authors recommend using the part of the releasing curve for which it holds: $M_t/M_\infty < 0.60$. For our analysis, we considered the initial stage of the release, corresponding to ELISA results of 3 hours, 24 hours, 48 hours and 72 hours release.

Constraints were applied to the exponent of release n and to the constant of apparent release K. Explanation of the choices for boundary conditions and constraints can be found in Section 7.1 of the Supporting Information.

RELEASE MODEL	*MECHANISM OF RELEASE*	*EXPONENT OF RELEASE (n)*	*TIME DEPENDENCE*
Fickian diffusion	Diffusion	0.5	$t^{0.5}$
Anomalous (non-Fickian) diffusion	Diffusion and swelling	0.5 < n < 1.0	t^{n-1}
Case II transport	Stress-induced relaxation of polymeric chains (swelling)	1.0	time independent
Super Case II transport	Break of polymeric network	n > 1.0	t^{n-1}

Table 2 Korsmeyer-Peppas diffusional release mechanisms from polymeric networks with a planar geometry.

2.6.2.2 Contribution of diffusion and relaxation

When release is not ascribable to neither diffusion nor swelling, it is defined as anomalous. To quantify the contribution these two phenomena have on anomalous transport we used the heuristic Peppas-Sahlin model [45]:

$$F = \frac{M_t}{M_\infty} = K_d \cdot t^m + K_r \cdot t^{2m} \quad (2)$$

The first term of equation (2) represents the Fickian diffusion contribution while the second one is the release due to swelling; *m* is the purely Fickian diffusion exponent.
The contribution of relaxation over diffusion can be obtained through the ratio:

$$\frac{R}{F} = \frac{K_r}{K_d} \cdot t^m \quad (3)$$

To calculate the parameters K_d, K_r and *m* we used a non-linear fitting method with the following constraints (explained in Section 7.2 of the Supporting Information):

- Coefficient of diffusion: $K_d \geq 0$;
- Coefficient of relaxation: $K_r \geq 0$;
- Fickian diffusion exponent m: $0.43 \leq m \leq 0.5$

2.6.3 Cellular response following TGF-β delivery

Presence of active TGFβ-3 was determined using TGFβ-reporter cells and a Luciferase Assay System (Kit E1501, Promega). The luciferase assay relies on the ability of $(CAGA)_9$ MLP-luc transfected cells to express luciferase upon TGF-β binding to its receptor TGFβR-II. When the Smad3/4 heterocomplex enters into the nucleus, it binds to its specific CAGA sequence placed upstream the luciferase reporter gene and causes its transcription in a dose responsive manner. Luciferase then oxidises the luciferin present into the assay kit in a chemical reaction in which part of the energy released is in form of light and can thus be detected by the luciferase assay (Figure 9). This assay represents a non-toxic, easy and inexpensive technique as well as one of the most efficient yet sensitive bioluminescent assay to detect presence of drugs in treated cells [46].

2.6.3.1 Determination of optimal incubation time

To determine the time reporter cells needed to uptake TGF-β and transcript luciferase, we performed a preliminary assay to assess the optimal incubation time. Reporter cells were seeded in a 24-well

plate at high density (100000 cells/well) and incubated for 3, 6 and 24 hours with 1ng/mL TGF-β dissolved in 500µL DMEM, supplemented with 10% FBS and 1% P/S. Following incubation, cells were assayed with Luciferase Assay System according to the manufacturer instructions. Highest values of luciferase determined our optimal incubation time.

2.6.3.2 Luciferase assay

Reporter HT1080 cells were seeded at a density of 50000 cells/well in a 24-well plate and allowed to adhere and grow at 37°C and 5% CO_2 for two days. At day 3, we isolated 100µL of conditioned medium and we diluted it in 400µL of fresh medium (10mg/mL BSA in serum-free DMEM) for a total volume of 500µL. Reporter cells were then incubated with diluted conditioned media for 6 hours at 37°C and 5% CO_2. Then, cells were lysed with 50µL lysis buffer – prepared by dissolving protease inhibitor and Tergitol-type nonyl phenoxypolyethoxylethanol (NP40) in a 1:25 ratio – and assayed with Luciferase Assay System according to the manufacturer instructions.

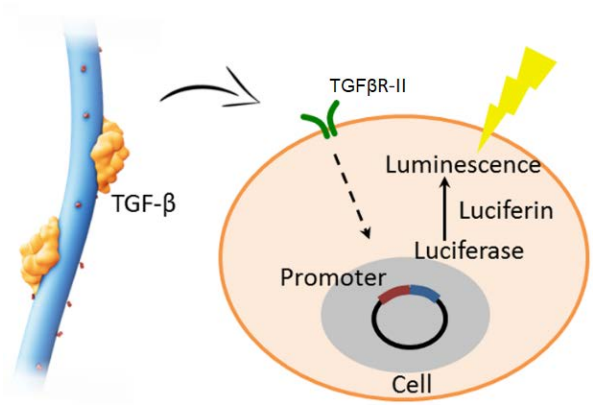

Figure 9 Activation of the SMAD signalling pathway upon TGF-B binding to its receptor TGFBR-II causes transcription of luciferase in a dose responsive manner. Luciferase then reacts with luciferin, causing its oxidation in a chemical reaction that produces a detectable luminescent signal. Adapted from [47].

2.7 TGF-β activity

Confirmation of TGF-β activity following delivery from UPy-PEG was assessed in epithelial cells through Western Blot and quantitative polymerase chain reaction (qPCR) assays. Active TGF-β can signal through its canonical pathway and phosphorylate SMAD2. Furthermore, it can stimulate epithelial cells to undergo EMT, increasing the expression of genes involved in this transition.

2.7.1 Phosphorylation of SMAD2

Western Blot on epithelial cells was performed according to the protocol by Mahmood and Yang [48]. To ensure reproducibility, the experiment was repeated three times in independent replications (labelled as T1, T2, T3).

2.7.1.1 Sample preparation

At day 1, epithelial cells were seeded at a density of 35000 cells/well in a 12-well plate and allowed to adhere and grow at 37°C and 5% CO_2 for 2 days. At day 3, cells were starved for 3 hours in serum-free DMEM and then incubated for 1 hour at 37°C and 5% CO_2 with conditioned medium and control medium as described in Table 3 and Table 4.

Following 1 hour of incubation, cells were lysed for total protein extraction with 50µL lysis buffer, prepared as a solution of protease inhibitor and phosphatase inhibitors in radioimmunoprecipitation (RIPA) buffer. Homogenates were size-fractionated on 10% polyacrylamide gel electrophoresis (PAGE) gels and transferred to polyvinylidene difluoride (PVDF) membranes. Membranes were blocked against non-specific binding sites with a solution of 5% BSA in TBST for 30 minutes at room temperature. Then, they were incubated overnight at 4°C with 0.2µL/mL anti-pSmad2 primary antibody (Rabbit antibody, Cell Signaling, Cat. No.: 3108) in 5% BSA in TBST. Next, membranes were incubated for 1 hour at room temperature with horseradish peroxidase (HRP)-labelled secondary antibody (Donkey anti-rabbit antibody, ThermoFisher Scientific, Cat. No.: 31458) dissolved at 0.1µL/mL concentration in a solution of 10% milk in TBST. Activity of HRP was detected through WesternBright™ Quantum detection kit (Advansta) and visualised by developing the membranes in the dark room using X-Ray films (Super RX films, Fujifilm).

SAMPLE NAME	*COMPOUND IN UPy-PEG*	*RELEASING TIME*
UPy-TGFβ 24h	TGF-β (25ng/mL)	21h
UPy-TGFβ 7d	TGF-β (25ng/mL)	141h

Table 3 Test sample conditions for Western Blot experiments. UPy-PEG containing TGF-β was formed as described in Section 2.4 and allowed to release for the time indicated in column "Releasing time". Then, epithelial cells were incubated with conditioned media for 1 hour before assaying with Western Blot.

SAMPLE NAME	*COMPOUND IN MEDIUM*	*DILUTION MEDIUM*
TGFβ	TGF-β (5ng/mL)	10mg/mL BSA in serum-free DMEM
SB	SB (50µM); TGF-β (5ng/mL)	10mg/mL BSA in serum-free DMEM
CTRL	/	10mg/mL BSA in serum-free DMEM

Table 4 Control sample conditions for Western Blot experiments. Compounds were dissolved in "Dilution medium" at concentrations indicated in column "Compound in medium". Epithelial cells were then incubated with control media for 1 hour and then assayed with Western Blot.

2.7.1.2 Loading control

To confirm equal protein loading across the gel and correct differences in protein concentration, it was performed a loading control with γ-Tubulin.
PVDF membranes were blocked against non-specific binding sites and then incubated overnight at 4°C with anti-γ-Tubulin (Mouse antibody, Sigma, Cat. No.: T6557) dissolved in a solution of 5% BSA/TBST at 0.1µL/mL concentration. To detect primary antibody activity, membranes were then incubated with anti-mouse HRP-labelled secondary antibody (Sheep anti-Mouse, GE Healthcare Life Sciences, Cat. No.: RPN4201) dissolved at 0.1µL/mL concentration in 10% milk/TBST solution and visualised with WesternBright™ Quantum detection kit.

2.7.2 Epithelial-to-Mesenchymal Transition (EMT)

Epithelial cells were stimulated to undergo EMT through incubation with conditioned medium for 3 days, following which they were detected for analysis. To ensure reproducibility, the experiment was repeated four times in independent replications (R1, R2, R3, R4).

At day 1, epithelial cells were seeded at a density of 2500 cells/well in a 12-well plate and incubated at 37°C and 5% CO_2. At day 2, culturing medium was replaced with conditioned medium and control medium, supplemented with 10% FBS (Table 5 and Table 6). At day 4 cells were observed under inverted microscope (Nikon Eclipse T*i*) and imaged. At day 5 cells were lysed with 100µL BL + TG buffer, prepared by dissolving 1-Thioglycerol (TG) in BL buffer at a 1:100 ratio. The plate was then stored at (-22°C) until qPCR analysis.

SAMPLE NAME	*COMPOUND IN UPy-PEG*	*RELEASING TIME*
UPy-TGFβ 3h	TGF-β (25ng/mL)	3h
UPy-TGFβ 24h	TGF-β (25ng/mL)	21h
UPy	/	24 h

Table 5 Test sample conditions for EMT experiments. UPy-TGFβ and UPy were formed as described in Section 2.4 and allowed to release for the time indicated in column "Releasing time". Epithelial cells were then incubated with conditioned media for 3 days before lysing.

SAMPLE NAME	*COMPOUND IN MEDIUM*	*DILUTION MEDIUM*
TGFβ	TGF-β (5ng/mL)	10mg/mL BSA in serum-free DMEM
CTRL	/	10mg/mL BSA in serum-free DMEM

Table 6 Control sample conditions for EMT experiments. Epithelial cells were incubated with control media for 3 days and then lysed.

2.7.2.1 Expression of mesenchymal markers

To confirm epithelial cells transition to the mesenchymal phenotype we looked at the expression of markers and transcription factors involved during EMT through quantitative polymerase chain reaction (qPCR). This assay ultimately confirmed TGF-β retained activity following delivery from UPy-PEG.

Lysed samples from EMT experiments were gradually thawed to room temperature. Pellets were scraped and pipetted into Eppendorf tubes for RNA purification and isolation, using the ReliaPrep™ RNA Cell Miniprep System (Promega Corporation). RNA concentration and purity were measured using NanoDrop® ND-1000 UV-Vis Spectrophotometer (Thermo Fisher Scientific). cDNA was made from purified RNA with the RevertAid First Strand cDNA Synthesis Kit (Thermo Scientific) and used for qPCR analysis.

Primers used for validation of EMT in epithelial cells were the following (sequences reported in Table 7):

- N-Cadherin (N-cad), mesenchymal cells marker;
- E-Cadherin (E-cad), protein highly expressed in epithelial tissue;
- Smooth muscle actin (SMA), cytoskeletal marker expressed when cells transition from cobble to spindle-shaped;
- Snail (SNAI-1), suppressor of E-cadherin expression during EMT;
- Slug (SNAI-2), transcriptional repressor of E-cadherin;
- β_2 microglobulin (B2M) and Glyceraldehyde 3-phosphate dehydrogenase (GAPDH), reference genes ubiquitously expressed in all tissues and cell types [49].

qPCR of these primers was performed in triplicates. A minus Reverse Transcription (-RT) control, containing four random reaction components except the reverse transcriptase, was included to test for contaminations in cDNA samples. As negative control a MilliQ® sample was used.

Data from qPCR were analysed through relative quantification method, also known as the $2^{-\Delta\Delta C_T}$ method, which related the PCR signal of the target genes to that of the reference genes [50].

GENE	***SEQUENCE***
N-Cadherin Forward	CAG ACC GAC CCA AAC AGC AAC
N-Cadherin Reverse	GCA GCA ACA GTA AGG ACA AAC ATC
E-Cadherin Forward	CCC GGT ATC TTC CCC GC
E-Cadherin Reverse	CAG CCG CTT TCA GAT TTT CAT
SMA Forward	CCG GGA GAA AAT GAC TCA AA
SMA Reverse	GAA GGA ATA GCC ACG CTC AG
Snail Forward	CCA GTG CCT CGA CCA CTA TG
Snail Reverse	CTG CTG GAA GGT AAA CTC TGG A
Slug Forward	CGG ACC CAC ACA TTA CCT TGT
Slug Reverse	TTC TCC CCC GTG TGA GTT CTA
B2M Forward	ACA CTG AAT TCA CCC CCA CT
B2M Reverse	GCT TAC ATG TCT CGA TCC CAC T
GAPDH Forward	AGC CAC ATC GCT CAG ACA C
GAPDH Reverse	GCC CAA TAC GAC CAA ATC C

Table 7 Sequences of forward and reverse primers used in qPCR to confirm EMT in epithelial cells.

2.7.2.1.1 Criteria of exclusion

For each sample's triplet, the coefficient of variation (CV) was calculated as the ratio between the standard deviation and the mean of the triplet's threshold cycle (C_T) values, multiplied by 100. C_T values which gave a CV higher than 2.0 were excluded from the analysis.

2.8 Statistics

To ensure reproducibility, data were obtained from at least two independent experiments (unless stated otherwise) and are presented as mean ± standard deviation (SD). Where applicable, statistically significant differences between the control group and the experimental groups were determined using a two-tailed paired Student's *t*-test. Probabilities of $P \geq 0.05$ were considered to be not statistically significant and were labelled as "n.s."; $P < 0.05$ is depicted with *, $P < 0.01$ with ** and $P < 0.001$ with ***. All statistical analyses were performed using Microsoft Office Excel.

3 Results

3.1 TGF-β solubility

Hydrophobicity of TGF-β and possible losses following addition in non-optimal solutions required a preliminary experiment to determine the best conditions for TGF-β detection. Our results showed that absence of BSA in solution resulted in high losses (Figure 10). The highest luciferase signal was measured in the sample where TGF-β was dissolved in 10mg/mL BSA in serum-free DMEM. Therefore, this constituted the preferred solution in every experiment involving TGF-β.

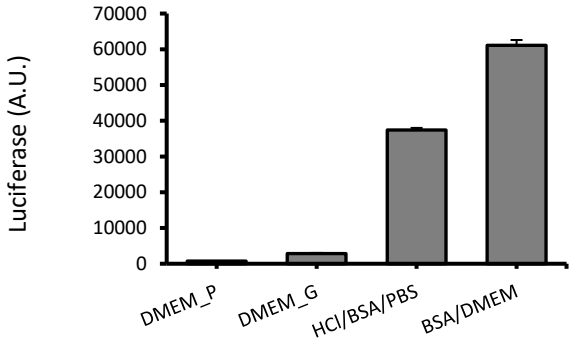

Figure 10 Comparison of TGF-β losses in different solutions. When TGF-β is added to a solution of serum-free DMEM in a polystyrene well plate it results in high losses (DMEM_P). The same happens by switching to a glass culture dish (DMEM_G). When the dilution solution was changed to 4mM HCl in 0.1% BSA in PBS results dramatically improve (HCl/BSA/PBS), being maximized in 10mg/mL BSA in DMEM (BSA/DMEM).

3.2 Quantification of UPy-TGFβ release

To determine the quantity of TGF-β delivered by UPy-TGFβ over time we performed three independent ELISA assays (P1, P2, P3). Results showed a common releasing profile between different experiments, which gradually decreased over time (Figure 11). Interestingly, the amount of TGF-β released differed consistently from experiments P1 and P2 to experiment P3. Of the initial 25 ng/mL TGF-β added to UPy-PEG during formation, at day 1 we found 0.47±0.17 ng/mL TGF-β in P1, 0.27±0.03 ng/mL in P2 and 1.81±0.04 ng/mL in P3. At day 2, while for P1 and P2 there was a decrease in the release (0.19±0.03 and 0.16±0.01 ng/mL respectively), in experiment P3 it remained quite stable (1.85±0.02 ng/mL). From day 3, all experiments showed a decreasing trend. At day 7, the amount of TGF-β released in P1 and P2 was very low while in P3 was still consistent (0.09±0.00 vs. 1.04±0.02). At day 14, when release for gel in P2 was over (0.04±0.00), UPy-TGFβ in P3 kept delivering (0.41±0.01), until day 21 when we considered reached the end of the release (0.05±0.01).

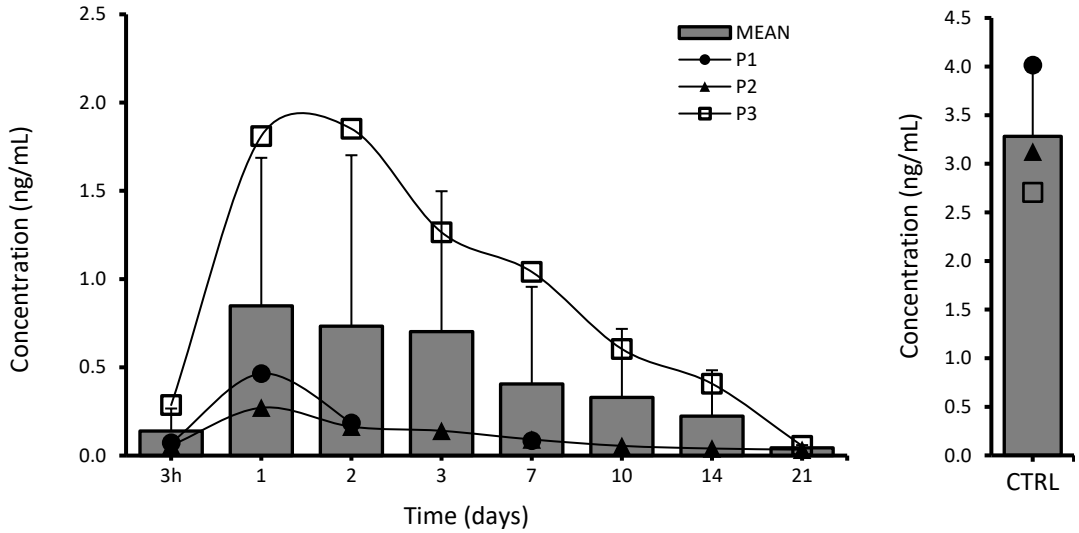

Figure 11 UPy-TGFβ releasing profile analysed through enzyme-linked immunosorbent assay (ELISA). Each column represents the average TGF-β delivered from the gel during three independent experiments (P1, P2, P3) over time. Release was monitored throughout 3 weeks and assayed at significant time points from the beginning of the experiment (x-axis). Each time point contains releasing products of one day release. The column on the right represents the positive control (CTRL), consisting of TGF-β dissolved at a concentration of 1 ng/mL in 10mg/mL BSA/serum-free DMEM. All results were corrected for the negative control (10mg/mL BSA dissolved in serum-free DMEM).

3.3 Release mechanism

Release mechanism constitutes an important parameter to classify a drug delivery system. Literature presents several methods to study release kinetics and the semi-empirical Korsmeyer-Peppas model represents one of the gold standards to analyse the behaviour of polymeric matrices.

Outcomes of the analyses revealed that release occurred through non-Fickian or anomalous transport (Table 8). Korsmeyer-Peppas fitting curves of TGF-β cumulative release for experiments P1, P2 and P3 can be found in Figure 18 in Section 7.3 of the Supporting Information.

EXPERIMENT	***K***	***n***	***R^2***
P1	0.062	0.642	0.9912
P2	0.039	0.651	0.9987
P3	0.157	0.823	0.9990

Table 8 Parameters of the Korsmeyer-Peppas model for experiments P1, P2 and P3. The exponent of release n indicated release due to anomalous transport (0.5 < n < 1). K is the kinetic constant which characterises the UPy- TGF-β system. Coefficients of determination R^2 indicated that the models provided a good approximation of the results ($R^2 \approx 1$).

To determine the contribution that diffusion and polymer chains relaxation had on the release we repeated the analyses with the Peppas-Sahlin heuristic model (characteristic parameters and fitting curves are reported in Table 10 and Figure 19 respectively of Section 7.4 of the Supporting Information). Our results highlighted that in P1 and P2 both diffusion and matrix relaxation contributed to the release, while in P3 relaxation was already predominant following the first three hours of the release (Table 9).

TIME (hours)	***R/F (experiment P1)***	***R/F (experiment P2)***	***R/F (experiment P3)***
0	0	0	0
3	0.5	0.4	6.4
24	1.1	1.0	15.7
48	1.5	1.4	21.1
72	/	1.6	25.1

Table 9 Relaxation-diffusion ratio for experiments P1, P2 and P3. Ratio R/F≤1.0 indicates release due to diffusion, while R/F>1.0 indicates a release due to relaxation. In P1 during the first 3 hours of the experiment release occurred through diffusion of TGF-β in the releasing medium, while after 24 hours it was controlled by relaxation of the UPy-PEG structure. In P2, we observed a more prolonged diffusion of TGF-β, which lasted for the first 24 hours, after which release was due to relaxation. In P3, the relaxation-diffusion ratio was greater than 1.0 for all the tested time points, indicating that release was mainly governed by relaxation of the UPy-PEG polymeric chains.

3.4 TGF-β activity in reporter cells

3.4.1 Determination of the luciferase optimal incubation time

Identification of the optimal incubation time allowed us to determine under which conditions we could get the highest signal for subsequent luciferase experiments. The best response was obtained after 6 hours of cells incubated with conditioned medium (Figure 12), which was therefore chosen as incubation time for following luciferase experiments.

3.4.2 Luciferase transcription in reporter cells

TGFβ-induced transcription of luciferase in reporter cells was measured in three independent experiments (P1, P2, P3) through luciferase assay. We could observe bioluminescence in all

experiments, obtaining a first proof of principle of TGF-β retained activity following delivery (Figure 13). In P1 luciferase was detected only in the first three days of the delivery, after which we obtained no cellular response, while for P2 and P3 luminescence was measured throughout the entire duration of the experiments.

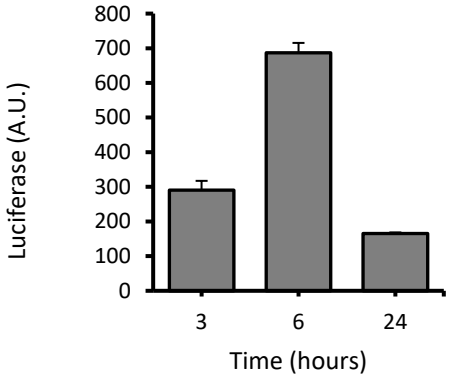

Figure 13 Luciferase assay for different incubation times. The highest luciferase signal was obtained after 6 hours incubation (687±28.7). Incubation of reporter cells with TGF-β conditioned medium for 3 hours and 24 hours gave a fluorescence of 291±26.6 and 165±3.1 respectively.

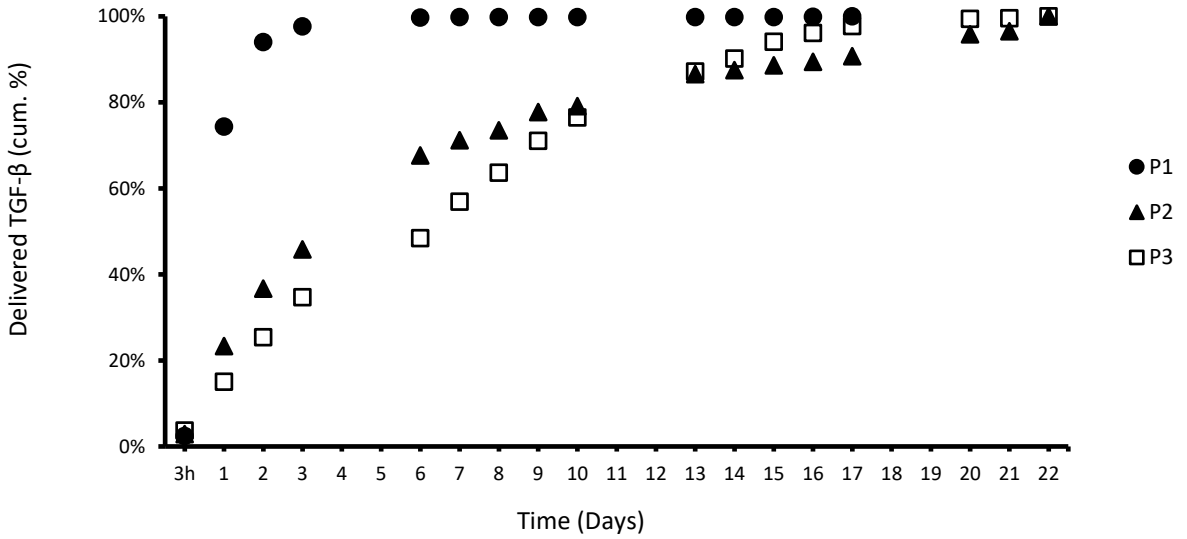

Figure 12 UPy-TGFβ release of three independent experiments (P1, P2, P3) analysed through luciferase assay. Results, corrected for the background, show the cumulative TGF-β released by UPy-TGFβ as a percentage of the total amount released by the gel in the same experiment. In P1, we measured fluorescence during the first three days, after which no cells activity was recorded. In P2 luciferase was measured in all samples until day 22, while in P3 we detected luminescence continuously until day 17.

3.5 Effect of UPy-TGFβ release on epithelial cells

3.5.1 Activation of TGF-β canonical signalling pathway

To test the capacity of UPy-PEG to deliver TGF-β in its active form, we assayed TGF-β ability to signal through its canonical pathway and phosphorylate SMAD2 in epithelial cells in three independent experiments (T1, T2, T3). Western blot results revealed significant amount of SMAD2 phosphorylation in cells treated with conditioned media compared to untreated cells (Figure 14; UPy-TGFβ24h = 7.02 ± 0.99, UPy-TGFβ7d = 5.53 ± 0.46). As expected, phosphorylation of SMAD2 was inhibited when an ALK5 kinase inhibitor SB was added to the culturing medium (1.28±1.02).

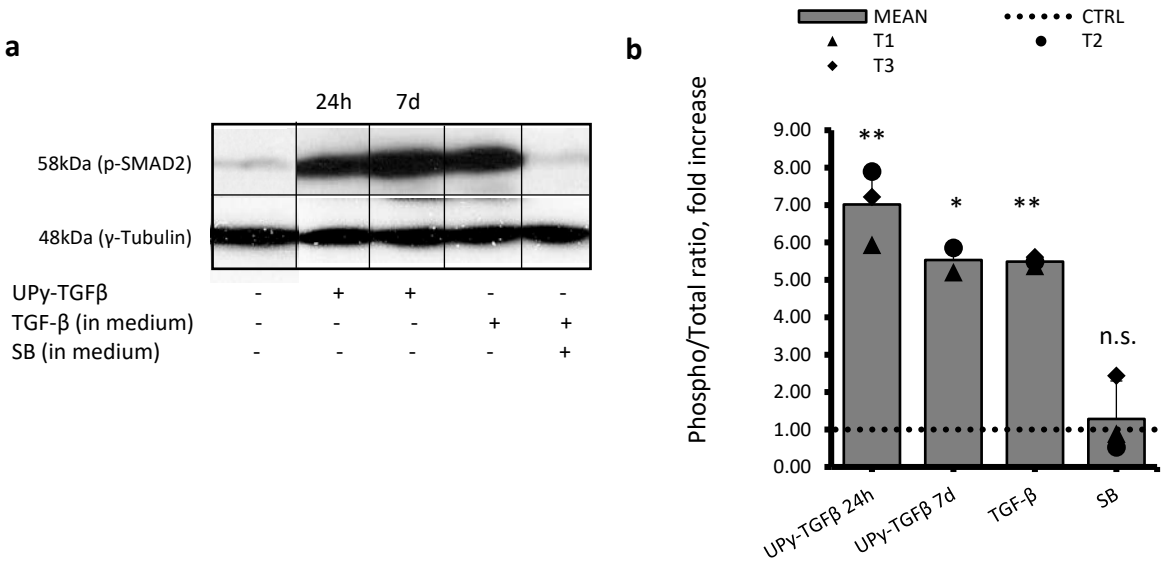

*Figure 14 Effect of TGF-β delivery in epithelial cells. a) Representative Western blot results. Following incubation with conditioned media from UPy-TGFβ releasing experiments, epithelial cells increased expression of SMAD2 compared to untreated cells. Equal protein loading was confirmed by detection of equal content of γ-Tubulin in cells. b) Densitometric analysis of Western blots. The graph represents data from three different independent experiments (T1, T2, T3) expressed as the ratio of phosphorylated to total protein signal intensity. Data are normalised for the untreated cells (CTRL), represented in the graph as a dotted line. The bars (MEAN) show the average SMAD2 phosphorylation of the three experiments and the error is represented as ± SD. Statistical analysis between each condition and the control (CTRL) was performed through paired Student's t test (df = 1 for UPy-TGFβ 7d; df = 2 for all the other samples). Asterisks indicate significant increase compared to control (n.s. not significant, P ≥ 0.05; *P < 0.05; **P < 0.01).*

3.5.2 Stimulation of EMT in epithelial cells

Evaluation of UPy-TGFβ effect on epithelial cells was meant to provide a further proof of the retained activity of TGF-β following delivery from UPy-PEG gel. After 2 days stimulation, we observed a change in cells morphology and reorganisation of the stress fibres (Figure 15). Incubation resulted in cells displaying the typical mesenchymal spindle shape in contrast with the cobblestone shape of cells treated with conditioned medium from simple UPy-PEG (UPy).

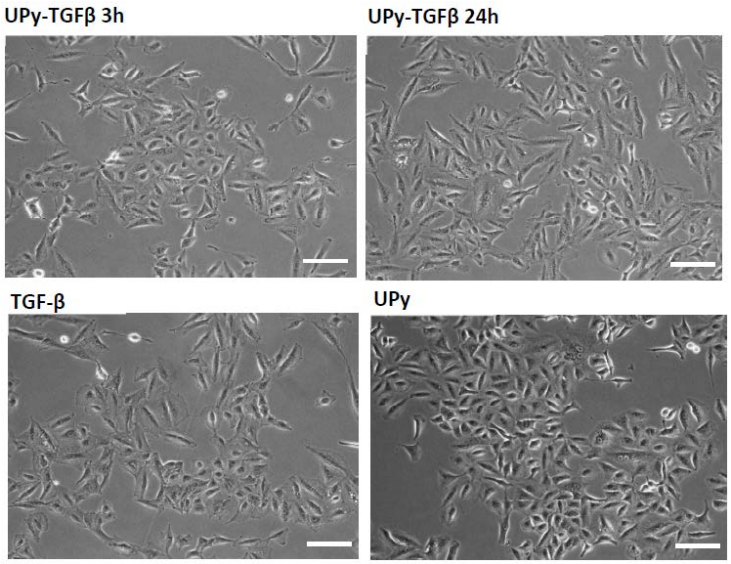

Figure 15 Effect of UPy-TGFβ on epithelial cells. Cells were treated for 3 days with conditioned medium from UPy-TGFβ releasing experiment of 3 hours and 24 hours. After 2 days incubation, we observed a change in morphology in cells treated with UPy-TGFβ compared to cells incubated with UPy-PEG with any TGF-β added (UPy). While in their normal state epithelial cells appear cobble-shape, when treated they lose this phenotype to acquire the mesenchymal spindle-like morphology. Scale bar = 100 µm.

3.5.2.1 Expression of EMT related genes

To confirm EMT transition in epithelial cells treated with conditioned media, we evaluated genes expressed by these cells through quantitative polymerase chain reaction (qPCR). Although not statistically significant, after 3 days incubation we observed a common tendency in upregulation of mesenchymal cell markers Neural cadherin (N-Cad), Snai-1 (Snail), Snai-2 (Slug) and smooth muscle actin (SMA) and downregulation of epithelial cadherin (Figure 16). This behaviour is a characteristic of EMT and corresponds to the change in morphology observed in epithelial cells.

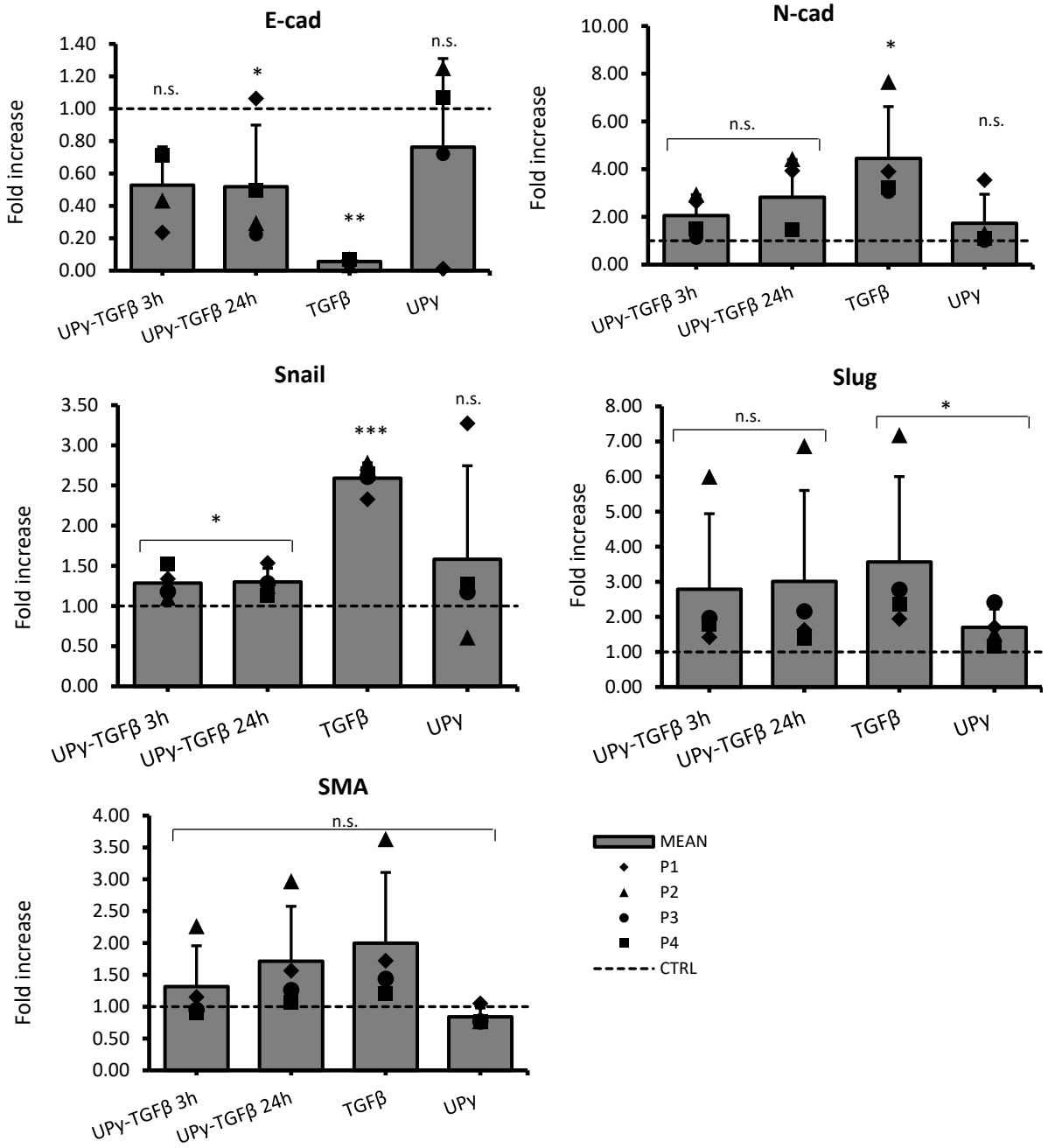

*Figure 16 Expression of EMT-related genes by epithelial cells treated with conditioned media from UPy-TGFB release. Values are corrected for the reference genes B2M and GAPDH and normalised for untreated cells (CTRL), reported in the graphs as a dotted line. Stimulation of cells with UPy-TGFβ significantly upregulated expression of Snai-1. Cells treatment with UPy-TGFβ24h resulted in decreased expression of E-cadherin (E-cad) compared to control. Upregulation of smooth muscle actin (SMA), Snai-2 and N-cadherin (N-cad) in treated cells was not statistically significant. The bars (MEAN) show the average expression for the four experiments and the error is represented as ± SD. Statistical analysis between each condition and the control (CTRL) was performed through paired Student's t test (df = 3; n.s., not significant, P ≥ 0.05; *P < 0.05; **P < 0.01, *** P < 0.001).*

4 Discussion

This research project aimed at demonstrating the efficacy of an injectable, pH-responsive hydrogel as drug carrier to stimulate epithelial-to-mesenchymal transition (EMT) in the epicardium. The tested hydrogel was a PEG-based polymer end-modified with supramolecular Ureido-pyrimidinone (UPy) groups, which provided the covalent PEG-based structure characteristics of injectability and pH-responsiveness. We probed the ability of UPy-PEG to deliver TGF-β, which was added during gel formation and has been used as a potent stimulator of EMT in epithelial cells. Validation occurred in three different phases: first, we determined the ability of UPy-PEG to release the TGF-β added to its structure during formation. Then, we studied the reproducibility of the delivery as well as its characteristics. Finally, we verified the activity of TGF-β following release by looking at its ability to signal through its canonical pathway. TGF-β signalling translated into transcription of luciferase in CAGA-responsive cells and stimulation of epithelial-to-mesenchymal transition in epithelial cells. Our results confirmed UPy-PEG as an effective carrier of TGF-β in cellular applications and demonstrated reproducibility of the delivery throughout different experiments. We further proved that TGF-β retained its potential following release and it was able to activate the SMAD signalling pathway and exert its effect both on reporter and epithelial cells.

To our knowledge, this represents a novel work in this context and this study the first step towards validation of a new approach to achieve epicardial stimulation through exogenous administration of TGF-β. UPy-PEG represents a key element of this therapy, offering stability to the growth factor in the harsh environment of the heart, constantly subjected to blood flow and pumping action. Moreover, it allows to specifically target the injured area, due to its fast response to pH changes and its rapid solidification. These characteristics are crucial when the compound to be delivered has a pleiotropic effect, as it holds for TGF-β (reviewed in [51]). Indeed, a time-planned target delivery of TGF-β to the site of interest may induce the desirable outcomes without the risk of harmful side effects. In this scenario, accurate responsiveness of the DDS to external stimuli acquire particular importance. Our experiments demonstrated UPy-PEG efficient transition from liquid to solid following pH changes; indeed, neutralization of the pH caused its rapid gelification. However, the supramolecular interactions responsible of the fast pH-responsiveness also determined the gel sensitivity to temperature changes [52]. Therefore, we adjusted the protocol of UPy-PEG formation to account for this dependence. Directly after formation at 70°C, UPy-PEG appeared as a liquid solution easy to pipet and transfer to well inserts. Addition of TGF-β required the reduction of the temperature to prevent its denaturation and loss of functionality [53]. However, UPy hydrogelator transitions from liquid to hydrogel below 50°C [54], thus working at room temperature caused its viscosity to rapidly rise. This may have impaired homogeneous distribution of TGF-β into the hydrogel matrix as well as the subsequent gel pipetting into well inserts. Therefore, we set the working temperature to 50°C, which prevented TGF-β degradation and UPy-PEG increase in viscosity.
Due to this temperature dependence, the process of UPy-PEG formation was extremely delicate and required to work fast. Moreover, it introduced an additional variable to carefully take into account during experimental planning. Previous *in vivo* studies addressed the issue by designing a custom-made technology that reduced the force required for injection [55]. However, this makes the procedure less straightforward and adds additional costs to it. A feasible yet convenient solution can come from a different UPy-PEG formulation method. As suggested by Dankers and colleagues in a previous study, *ex vivo* studies should opt for milder formulation conditions like the ones offered by the "*temperature method"* [56]. This technique allows the gel to easily flow into an injection syringe without the viscosity limitations coming from the pH formation method used in our experiments.

The second phase of UPy-PEG validation as delivery system consisted in the analysis of its release performance. Our ELISA results demonstrated the gel ability to release TGF-β over time. We

observed the same trend throughout three different experiments, confirming the reproducibility of the delivery. However, we reported variability in terms of quantity of TGF-β released and duration of the delivery. In the attempt to understand the reasons for this behaviour, we analysed UPy-PEG kinetics of release with the Korsmeyer-Peppas semi-empirical model. According to this model, release can be classified as Fickian or non-Fickian, depending on the mechanism which governs delivery (extensively described in [57]). If release occurs through diffusion of the encapsulated molecule in the releasing medium it is defined as Fickian, while when it is driven by relaxation of the polymeric chains (swelling) it is referred as non-Fickian. In the latter case, as the hydrogel swells and water enters into the matrix, the compound leaves the hydrogel structure and goes into the releasing medium [57]. When delivery does not pertain to any of these two cases, it is categorised as anomalous, meaning that both phenomena of diffusion and swelling participate in the delivery of the compound and their contribution can be obtained through the Peppas-Sahlin model. Results of our analysis showed that TGF-β delivery occurred through anomalous transport. Moreover, in P1 and P2 diffusion was responsible of the release during the first hours (3 and 24 respectively) of the experiments, after which the releasing rate was controlled by UPy-PEG swelling. On the other hand, in P3 hydrogel relaxation was already predominant after three hours from the beginning of the experiment.

The simultaneous contribution of diffusion and swelling in the release of drugs from polymeric matrices is frequently reported in literature. Moreover, when the compound is hydrophobic, there is high chance that the physical interactions with the hydrogel matrix influence the release kinetics [54]. Hendrikse and colleagues hypothesized that the interactions that occurred between TGF-β and UPy-PEG are of electrostatic nature and can change the rate at which the medium is absorbed by the hydrogel matrix and TGF-β presented to cells [47]. Furthermore, the dynamic crosslinks that characterise UPy-PEG matrix, together with drug size, crosslink density, swelling ratio, tortuosity of the hydrogel structure, might have been all factors responsible for the variability observed in the gel releasing profile [54][60]. Our hypothesis is that the initial TGF-β diffusion resulted from the movement of the growth factor located near the surface, which was eased in escaping the hydrogel matrix. However, the majority of the release occurred when the gel started swelling and further continued as it degraded. We expect to retrieve all TGF-β added during formation upon complete UPy-PEG erosion [54].

It should be mentioned that some assumptions might have limited our study. First, we only used data from 3 hours, 24 hours, 48 hours and 72 hours of release. Indeed, the models used can give a good approximation of the results only if they are applied to the stage of the release where it holds $M_t/M_\infty < 0.60$. Inclusion of more information from the first stage of the delivery (i.e. from 1 hour, 2 hours, 6 hours, 12 hours time points) could probably help obtaining better results. Moreover, we assumed that TGF-β was homogeneously distributed in the hydrogel matrix and that the contact surface of UPy-PEG with the releasing medium was kept at constant TGF-β concentration. Despite putting particular attention in the process of hydrogel formation, we cannot exclude the role that viscosity could have played in ensuring TGF-β homogeneous distribution into UPy-PEG structure. Furthermore, the presence of hydrogen bonds, hydrophilic and hydrophobic groups as well as the UPy-PEG fibres network could all have constituted factors that caused a heterogenous movement of TGF-β into the medium. Finally, both Korsmeyer-Peppas and Peppas-Sahlin models do not consider mass transfer phenomena and mechanisms of medium permeation into the hydrogel. A more comprehensive analysis can be done by applying mechanistic theories that consider device geometry, mass transfer, medium movement, change of volume, distribution of the drug into the polymer matrix, heterogeneity of the matrix etc. [61]. However, even these theories do not provide the full picture of the situation, where hydrogel characteristics (i.e. pH-responsiveness, nature of the crosslinks, interactions between the drug and the matrix) also contribute to the delivery process. Nevertheless, despite the limitations that characterised our study, we were able to demonstrate UPy-PEG ability to deliver TGF-β in different experiments. Furthermore, we highlighted the contribution of diffusion and swelling to the release mechanism and the presence of interactions between the growth factor and the hydrogel matrix, which might have also influenced the delivery.

After confirming UPy-PEG as a TGF-β delivery system, we studied the activity of the growth factor in cells. Our findings proved that addition of the compound to basic UPy-hydrogelator did not compromise its activity and that, following delivery, TGF-β retained its ability to bind to its receptor TGFβR-II and signal through its canonical pathway. TGF-β signalling produced significant SMAD2 phosphorylation in epithelial cells and caused transcription of luciferase in reporter cells. Moreover, stimulation of epithelial cells with UPy-PEG containing TGF-β caused cells to change their morphology and exhibit a more elongated, spindle shape, typical of the mesenchymal phenotype. Analysis of the genes expressed by these cells revealed a general increase in mesenchymal expression markers and a decrease in E-cadherin expression, that can explain the morphological change observed in treated cells. Although not statistically significant, these results demonstrated an effect of UPy-TGFβ towards induction of EMT in epithelial cells. The variability observed amongst different experiments could have multiple explanations. It is possible that, at the time of analysis, cells have already reached the density threshold which induce switch in the expression of Cadherins. Indeed, high cell-cell contact is known to cause increased expression of E-Cadherin and a decrease in N-Cadherin levels [62][63]. Furthermore, low expression of Snail and Slug can be related to the fact that SNAI transcription factors act upstream repression of the epithelial genes. In response to TGF-β, the SMADs complex activates and increases the activity of the EMT transcription factors, including Snail and Slug [64]–[66]. In turn, Snail and Slug repress transcription of the genes encoding E-Cadherin and activate genes that contribute to the mesenchymal phenotype. Therefore, in some experiments we might only have observed the effect of Snail and Slug activation, missing their actual upregulation. In addition, biological variability, non-optimal culturing conditions and errors during RNA isolation and cDNA synthesis are all factors that could also have contributed to the high standard deviation observed.

4.1 Future recommendations

Results of this *in vitro* study can represent a useful guideline for future *ex vivo* experiments. We showed the importance of temperature in the process of UPy-PEG formation. To prevent the change in viscosity that arises in response to temperature gradients, *ex vivo* studies should consider gel injection through syringes in a temperature-controlled environment, where UPy-PEG is sourced from a temperature controlled batch. Moreover, administration of small volumes of UPy-TGFβ would probably ease the procedure, lowering the force required for injection. Before usage, syringes could also be flushed with basic PBS that might help keeping the pH high and, thus, the gel in its liquid state. In alternative, one could also consider to form UPy-PEG through the temperature-based method, extensively described by Dankers et al. in [56].
It would be interesting to determine whether differences in experimental conditions from *in vitro* to *ex vivo* studies will influence the release kinetics. As previously mentioned, both Korsmeyer-Peppas and Peppas-Sahlin models could provide a better approximation of the delivery if more data from the early phase of the release become available. Moreover, it will be worth to verify if absence of the insert will allow the gel complete erosion and an increase in the amount of TGF-β delivered.

5 Conclusions

In conclusion, we demonstrated the ability of a pH-responsive Ureidopyrimidinone-based supramolecular polymer to release the incorporated growth factor TGF-β. We showed that, after pH neutralization, the hydrogel quickly solidified and became a reservoir of the carried compound. Drug diffusion and polymer swelling were two phenomena that contributed to the release, which was most probably also influenced by the electrostatic interactions between the crosslinked hydrogel

components. Following delivery, TGF-β retained its ability to signal through its SMAD canonical pathway, phosphorylate SMAD2 and activate transcription of luciferase in reporter cells. Epithelial cells treated with TGFβ-loaded UPy-PEG displayed a rearrangement of their stress fibres and a change in their morphology, exhibiting a more elongated and spindle shape. Although we found differences in gene expression – probably related to culturing conditions, biological variability, experimental timing, and to the assay procedure – UPy-TGFβ stimulation will mostly likely result in the induction of epithelial to mesenchymal transition in epithelial cells.

6 Acknowledgments

I'd like to thank Prof. Marie-José Goumans for offering me the opportunity to work in her lab at Leiden University Medical Center. Additionally, I want to thank Dr. Anke Smits for trusting my knowledge and giving me precious advises throughout the course of this Master thesis project. I especially want to thank Esther Dronkers for being an encouraging and patient supervisor. Thanks for giving me always interesting points of view and for stimulating my curiosity.

I'd like to express all my gratitude to my thesis advisor Dr. Lidy Fratila-Apachitei; thanks for being always extremely helpful with your comments and open to discuss any doubts and idea I came up with as well as for introducing me to Prof. Goumans.

After this journey, a special thank goes to my mother and my father. Being your daughter is the most precious gift I received from life. Thanks for teaching me the importance of commitment, curiosity and enthusiasm, and for making me so passionate about life.

I'd like to thank Enza for teaching me the importance of asking questions and dedicate time to silence and stillness, and Mariangela for being the most loyal and precious friend I have and for showing me your esteem and love when I need the most.

Finally, this journey wouldn't have been the same without *Marco*. Thank you for being the most supporting, encouraging and critic person of my life. You taught me devotion and inquisitiveness for my own work and you are ultimately the wisest, most generous and brilliant human I've ever met. Without you I'd have never become the researcher, but most importantly, the woman I am.

7 Supporting Information

7.1 Boundary conditions and constraints in Korsmeyer-Peppas model

The Korsmeyer-Peppas model requires some considerations to be done before the start of the analysis. As stated in Section 2.6.2.1, we assumed the following boundary conditions:

1) One-dimensional release through a thin slab;
2) Uniform TGF-β concentration into the system at t=0;
3) Constant TGF-β diffusivity through UPy-PEG.

The presence of the well-insert in our system mainly exposed one surface of UPy-TGFβ to the releasing medium. Indeed, due to the insert structure, release could only occur through the insert porous membrane in contact with the releasing medium. Moreover, the volume of medium added to each well was calculated to prevent it from entering the insert from the upper part. Therefore, we considered reasonable to assume that release occurred only in one, vertical, direction (Figure 17).
We further considered UPy-PEG as a thin slab, where release can only occur via the main surfaces. Indeed in our experiments, TGF-β movement was only allowed through the bottom surface since diffusion through the edges was prevented due to the presence of the insert.

Following TGF-β addition to UPy-PEG, we ensured mixing of the growth factor into the UPy matrix by stirring UPy-TGFβ at constant rate (550 rpm) for 10 minutes (Section 2.4). This procedure ensures uniform TGF-β distribution into the hydrogel matrix, thus its homogeneous concentration into the system before the start of the release.

Finally, we considered TGF-β movement into the releasing medium as a phenomenon occurring at constant rate, which allowed for a unique definition of the diffusion constant K, thus easing the analysis.

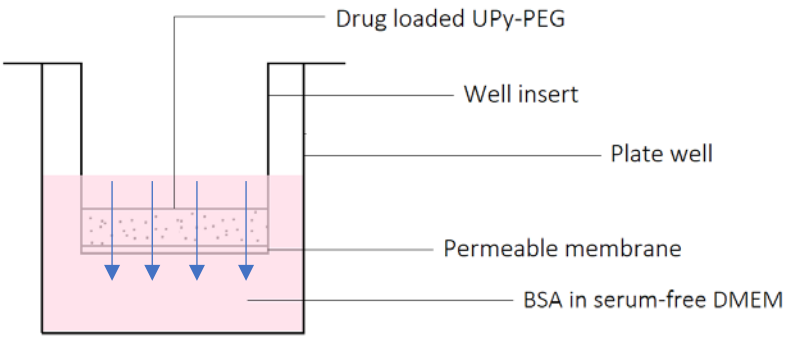

Figure 17 In vitro experimental layout. Arrows indicate the direction of the release.

Constraints applied to the exponent of release (*n*) were set according to what prescribed by Korsmeyer and Peppas in their study [44]. The constant of apparent release (*K*), proportional to the squared velocity of the diffusing particles (m^2/s), constitutes a measure of the speed of the phenomenon and, thus, it was imposed to be positive.

- $0.5 \leq n \leq 1.0$
- $K \geq 0$

7.2 Constraints in Peppas-Sahlin model

According to Peppas and Sahlin, regardless the geometry of the releasing device, the exponent of release can only vary between two extremes [45]. Therefore, we constrained *m* as recommended by the authors:

- $0.43 \leq m \leq 0.5$

The constant of diffusivity (K_d) and the constant of relaxation (K_r) were imposed to be positive since they provide information of the speed of the diffusion process (m^2/s):

- $K_d \geq 0$
- $K_r \geq 0$

7.3 Korsmeyer-Peppas fitting curves

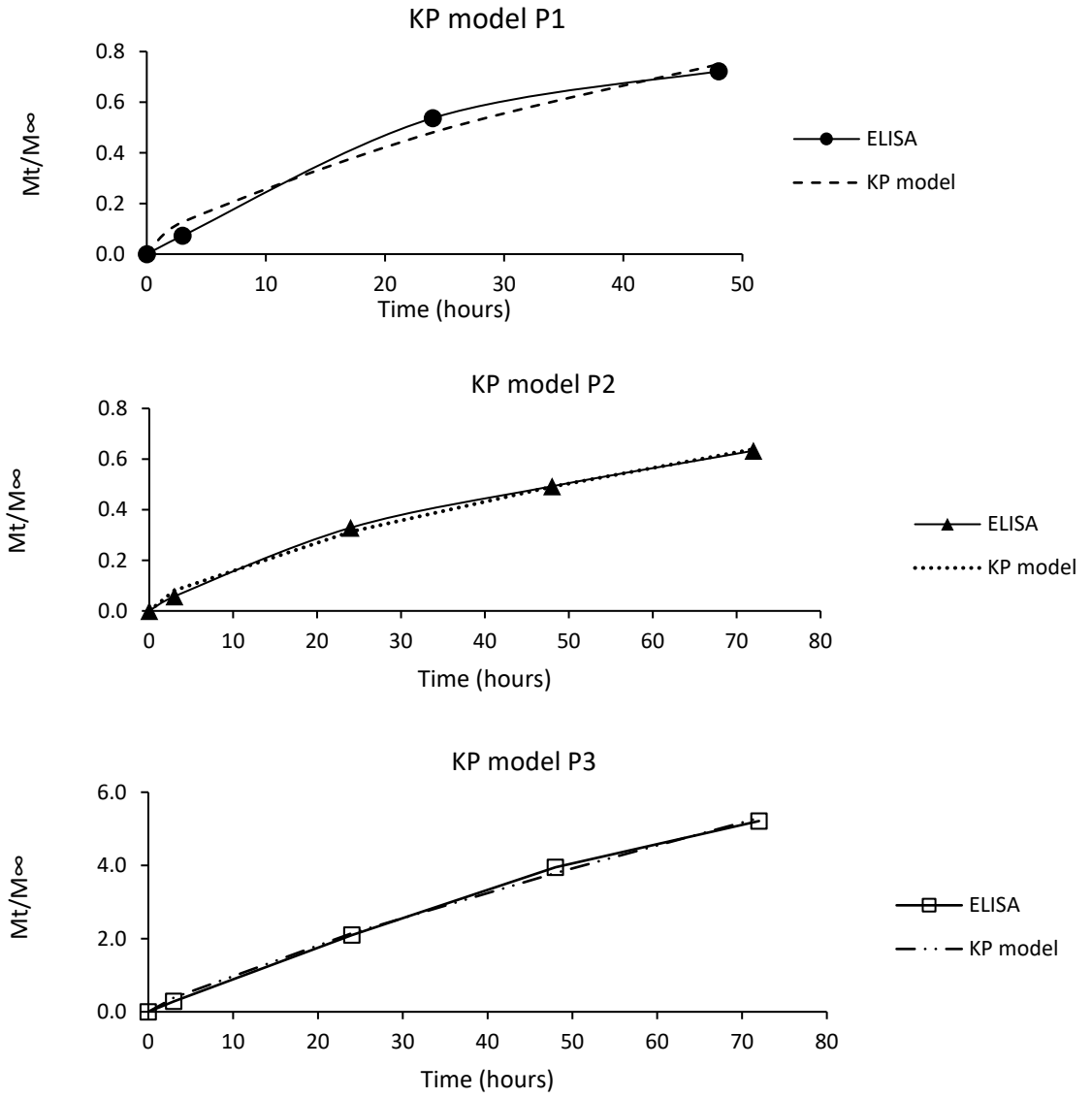

Figure 18 Korsmeyer-Peppas model of TGF-β release for experiments P1, P2 and P3. Each graph displays data from ELISA cumulative release and the fitting model for that experiment. F is the cumulative TGF-β release expressed in ng/mL, while time axis shows points from 3, 24, 48 and 72 hours release.

7.4 Peppas-Sahlin characteristic parameters and fitting curves

EXPERIMENT	K_d	K_r	*m*	R^2
P1	0.056	0.016	0.430	0.9886
P2	0.039	0.010	0.430	0.9976
P3	0.032	0.129	0.430	0.9988

Table 10 Release parameters of Peppas-Sahlin model for experiments P1, P2 and P3. Kd is the constant of diffusion, Kr is the constant of relaxation, m is the diffusion exponent and R^2 the coefficient of determination.

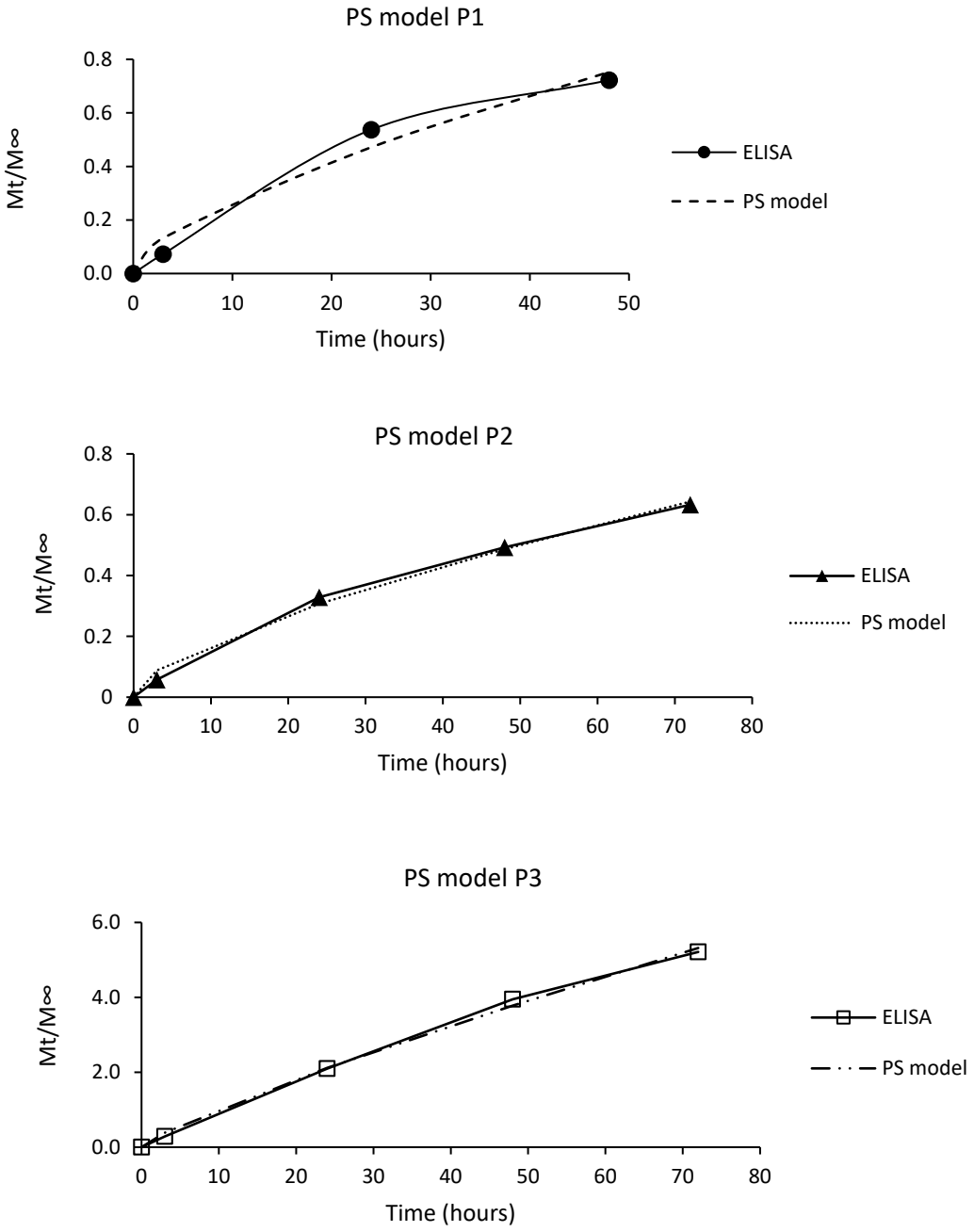

Figure 19 Peppas-Sahlin model of TGF-β release for experiments P1, P2 and P3. Each graph displays data from the ELISA assay and the fitting model for that experiment. F is the cumulative TGF-β release expressed in ng/mL, while the time axis shows points from 3, 24, 48 and 72 hours release.

Bibliography

[1] Wilkins E., Wilson I., Wickramasinghe K., Bhatnagar P., Leal J., Luengo-Fernandez R., Burns R., Rayner M., and Townsend N., *European Cardiovascular Disease Statistics 2017 edition*. 2017.

[2] S. Baer, "Acute myocardial infarction," *Journal of the American Medical Association*, vol. 118, no. 3. p. 248, 1942.

[3] G. Y. H. . Jackson, G.; Gibbs, C.R.; Davies, M.K.; Lip, "ABC of heart failure: Pathophysiology," *Br. Med. J.*, vol. 320, pp. 167–170, Jun. 2000.

[4] B. Ibanez, S. James, S. Agewall, M. J. Antunes, C. Bucciarelli-Ducci, H. Bueno, A. L. P. Caforio, F. Crea, J. A. Goudevenos, S. Halvorsen, G. Hindricks, A. Kastrati, M. J. Lenzen, E. Prescott, M. Roffi, M. Valgimigli, C. Varenhorst, P. Vranckx, P. Widimský, A. Baumbach, R. Bugiardini, I. M. Coman, V. Delgado, D. Fitzsimons, O. Gaemperli, A. H. Gershlick, S. Gielen, V. P. Harjola, H. A. Katus, J. Knuuti, P. Kolh, C. Leclercq, G. Y. H. Lip, J. Morais, A. N. Neskovic, F. J. Neumann, A. Niessner, M. F. Piepoli, D. J. Richter, E. Shlyakhto, I. A. Simpson, P. G. Steg, C. J. Terkelsen, K. Thygesen, S. Windecker, J. L. Zamorano, U. Zeymer, M. Chettibi, H. G. Hayrapetyan, B. Metzler, F. Ibrahimov, V. Sujayeva, C. Beauloye, L. Dizdarevic-Hudic, K. Karamfiloff, B. Skoric, L. Antoniades, P. Tousek, C. J. Terkelsen, S. M. Shaheen, T. Marandi, M. Niemela, S. Kedev, M. Gilard, A. Aladashvili, A. Elsaesser, I. G. Kanakakis, B. Merkely, T. Gudnason, Z. Iakobishvili, L. Bolognese, S. Berkinbayev, G. Bajraktari, M. Beishenkulov, I. Zake, H. Ben Lamin, O. Gustiene, B. Pereira, R. G. Xuereb, S. Ztot, V. Juliebø, J. Legutko, A. T. Timoteo, G. Tatu-Chit¸oiu, A. Yakovlev, L. Bertelli, M. Nedeljkovic, M. Studencan, M. Bunc, A. M. G. de Castro, P. Petursson, R. Jeger, M. S. Mourali, A. Yildirir, A. Parkhomenko, and C. P. Gale, "2017 ESC Guidelines for the management of acute myocardial infarction in patients presenting with ST-segment elevation," *European Heart Journal*, vol. 39, no. 2. pp. 119–177, 2018.

[5] S. A. Doppler, M. A. Deutsch, R. Lange, and M. Krane, "Direct reprogramming—The future of cardiac regeneration?," *Int. J. Mol. Sci.*, vol. 16, no. 8, pp. 17368–17393, 2015.

[6] H. K. Awada, M. P. Hwang, and Y. Wang, "Towards comprehensive cardiac repair and regeneration after myocardial infarction: Aspects to consider and proteins to deliver," *Biomaterials*, vol. 82. pp. 94–112, 2016.

[7] O. Bergmann, R. D. Bhardwaj, S. Bernard, S. Zdunek, F. Barnabé-Heide, S. Walsh, J. Zupicich, K. Alkass, B. A. Buchholz, H. Druid, S. Jovinge, and J. Frisén, "Evidence for cardiomyocyte renewal in humans," *Science (80-.).*, vol. 324, no. 5923, pp. 98–102, 2009.

[8] P. K. Nguyen, J.-W. Rhee, and J. C. Wu, "Adult Stem Cell Therapy and Heart Failure, 2000 to 2016: A Systematic Review.," *JAMA Cardiol.*, vol. 1, no. 7, pp. 831–841, 2016.

[9] A. Wessels, M. J. B. van den Hoff, R. F. Adamo, A. L. Phelps, M. M. Lockhart, K. Sauls, L. E. Briggs, R. A. Norris, B. van Wijk, J. M. Perez-Pomares, R. W. Dettman, and J. B. E. Burch, "Epicardially derived fibroblasts preferentially contribute to the parietal leaflets of the atrioventricular valves in the murine heart," *Dev. Biol.*, vol. 366, no. 2, pp. 111–124, Jun. 2012.

[10] M. Krainock, O. Toubat, S. Danopoulos, A. Beckham, D. Warburton, and R. Kim, "Epicardial Epithelial-to-Mesenchymal Transition in Heart Development and Disease," *J. Clin. Med.*, vol. 5, no. 2, p. 27, Feb. 2016.

[11] A. Von Gise and W. T. Pu, "Endocardial and epicardial epithelial to mesenchymal transitions in heart development and disease," *Circ. Res.*, vol. 110, no. 12, pp. 1628–1645, 2012.

[12] A. C. G. de Groot, E. M. Winter, and R. E. Poelmann, "Epicardium-derived cells (EPDCs) in

development, cardiac disease and repair of ischemia," *J. Cell. Mol. Med.*, vol. 14, no. 5, pp. 1056–1060, Apr. 2010.

[13] B. Zhou, F. X. Mcgowan, W. T. Pu, B. Zhou, L. B. Honor, H. He, Q. Ma, J. H. Oh, C. Butterfield, M. Qing, J. H. Oh, C. Butterfield, R. Z. Lin, J. M. Melero-Martin, E. Dolmatova, H. S. Duffy, A. Von Gise, P. Zhou, Y. W. Hu, G. Wang, B. Zhang, L. Wang, J. L. Hall, M. A. Moses, F. X. Mcgowan, and W. T. Pu, "Adult mouse epicardium modulates myocardial injury by secreting paracrine factors," *J. Clin. Invest.*, vol. 121, no. 5, pp. 1894–1904, 2011.

[14] B. van Wijk, Q. D. Gunst, A. F. M. Moorman, and M. J. B. van den Hoff, "Cardiac Regeneration from Activated Epicardium," *PLoS One*, vol. 7, no. 9, 2012.

[15] M. J. Goumans, T. P. de Boer, A. M. Smits, L. W. van Laake, P. van Vliet, C. H. G. Metz, T. H. Korfage, K. P. Kats, R. Hochstenbach, G. Pasterkamp, M. C. Verhaar, M. A. G. van der Heyden, D. de Kleijn, C. L. Mummery, T. A. B. van Veen, J. P. G. Sluijter, and P. A. Doevendans, "TGF-β1 induces efficient differentiation of human cardiomyocyte progenitor cells into functional cardiomyocytes in vitro," *Stem Cell Res.*, vol. 1, no. 2, pp. 138–149, Jun. 2008.

[16] A. T. Moerkamp, K. Lodder, T. van Herwaarden, E. Dronkers, C. K. E. Dingenouts, F. C. Tengström, T. J. van Brakel, M.-J. Goumans, and A. M. Smits, "Human fetal and adult epicardial-derived cells: a novel model to study their activation," *Stem Cell Res. Ther.*, vol. 7, no. 1, p. 174, 2016.

[17] M.-J. Goumans, G. Valdimarsdottir, S. Itoh, A. Rosendahl, S. Paschalis, and P. ten Dijke, "Balancing the activation state of the endothelium via two distinct TGF-beta type I receptors," *EMBO J.*, vol. 21, no. 7, pp. 1743–1753, Apr. 2002.

[18] G. Euler-Taimor and J. Heger, "The complex pattern of SMAD signaling in the cardiovascular system," *Cardiovascular Research*, vol. 69, no. 1. pp. 15–25, 2006.

[19] X.-H. Feng and R. Derynck, "Specificity and Versatility in TGF-β Signaling Through SMADs," *Annu. Rev. Cell Dev. Biol.*, vol. 21, no. 1, pp. 659–693, 2005.

[20] S. Campanaro, S. Picelli, R. Torregrossa, L. Colluto, M. Ceol, D. Del Prete, A. D'Angelo, G. Valle, and F. Anglani, "Genes involved in TGFβ1-driven epithelial-mesenchymal transition of renal epithelial cells are topologically related in the human interactome map," *BMC Genomics*, vol. 8, 2007.

[21] A. Masszi, G. Sirokmány, A. Kapus, L. Rosivall, J. Wang, C. Di Ciano, O. D. Rotstein, C. A. G. McCulloch, I. Mucsi, and W. T. Arthur, "Central role for Rho in TGF-β 1 -induced α-smooth muscle actin expression during epithelial-mesenchymal transition," *Am. J. Physiol. Physiol.*, vol. 284, no. 5, pp. F911–F924, 2015.

[22] A. Barrallo-Gimeno, "The Snail genes as inducers of cell movement and survival: implications in development and cancer," *Development*, vol. 132, no. 14, pp. 3151–3161, 2005.

[23] E. A. Carver, R. Jiang, T. Gridley, K. F. Oram, and Y. Lan, "The Mouse Snail Gene Encodes a Key Regulator of the Epithelial-Mesenchymal Transition," *Mol. Cell. Biol.*, vol. 21, no. 23, pp. 8184–8188, 2002.

[24] P. Savagner, K. M. Yamada, and J. P. Thiery, "The zinc-finger protein slug causes desmosome dissociation, an initial and necessary step for growth factor-induced epithelial-mesenchymal transition," *J. Cell Biol.*, vol. 137, no. 6, pp. 1403–1419, 1997.

[25] A. C. Tecalco-Cruz, D. G. Ríos-López, G. Vázquez-Victorio, R. E. Rosales-Alvarez, and M. Macías-Silva, "Transcriptional cofactors Ski and SnoN are major regulators of the TGF-β/Smad signaling

pathway in health and disease," *Signal Transduction and Targeted Therapy*, vol. 3, no. 1. 2018.

[26] J. F. O'Sullivan, A. L. Leblond, G. Kelly, A. H. S. Kumar, P. Metharom, C. K. Büneker, N. Alizadeh-Vikali, I. Hristova, B. G. Hynes, R. O'Connor, and N. M. Caplice, "Potent long-term cardioprotective effects of single low-dose insulin-like growth factor-1 treatment postmyocardial infarction," *Circulation: Cardiovascular Interventions*, vol. 4, no. 4. pp. 327–335, 2011.

[27] V. F. M. Segers and R. T. Lee, "Protein therapeutics for cardiac regeneration after myocardial infarction," *Journal of Cardiovascular Translational Research*, vol. 3, no. 5. pp. 469–477, 2010.

[28] L. Miquerol, B. L. Langille, and A. Nagy, "VEGF-A overexpression induces embryonic cardiopathy," *Development*, vol. 127, pp. 3941–3946, 2000.

[29] D. T. Wu, M. Bitzer, W. Ju, P. Mundel, and E. P. Bö, "TGF-Concentration Specifies Differential Signaling Profiles of Growth Arrest/Differentiation and Apoptosis in Podocytes," *J Am Soc Nephrol*, vol. 16, pp. 3211–3221, 2005.

[30] S. J. Bryant and K. S. Anseth, "The effects of scaffold thickness on tissue engineered cartilage in photocrosslinked poly(ethylene oxide) hydrogels," *Biomaterials*, vol. 22, no. 6, pp. 619–626, 2001.

[31] C. Tu, Q. Cai, J. Yang, Y. Wan, J. Bei, and S. Wang, "The fabrication and characterization of poly(lactic acid) scaffolds for tissue engineering by improved solid-liquid phase separation," *Polym. Adv. Technol.*, vol. 14, no. 8, pp. 565–573, 2003.

[32] K. Kadner, S. Dobner, T. Franz, D. Bezuidenhout, M. S. Sirry, P. Zilla, and N. H. Davies, "The beneficial effects of deferred delivery on the efficiency of hydrogel therapy post myocardial infarction," *Biomaterials*, vol. 33, pp. 2060–2066, 2012.

[33] A. S. Salimath, E. A. Phelps, A. V Boopathy, P.-L. Che, and M. Brown, "Dual Delivery of Hepatocyte and Vascular Endothelial Growth Factors via a Protease-Degradable Hydrogel Improves Cardiac Function in Rats," *PLoS One*, vol. 7, no. 11, p. 50980, 2012.

[34] M. M. C. Bastings, S. Koudstaal, R. E. Kieltyka, Y. Nakano, A. C. H. Pape, D. A. M. Feyen, F. J. van Slochteren, P. A. Doevendans, J. P. G. Sluijter, E. W. Meijer, S. A. J. Chamuleau, and P. Y. W. Dankers, "A fast pH-switchable and self-healing supramolecular hydrogel carrier for guided, local catheter injection in the infarcted myocardium," *Adv. Healthc. Mater.*, vol. 3, no. 1, pp. 70–78, 2014.

[35] P. Y. W. Dankers, T. M. Hermans, T. W. Baughman, Y. Kamikawa, R. E. Kieltyka, M. M. C. Bastings, H. M. Janssen, N. A. J. M. Sommerdijk, A. Larsen, M. J. A. Van Luyn, A. W. Bosman, E. R. Popa, G. Fytas, and E. W. Meijer, "Hierarchical formation of supramolecular transient networks in water: A modular injectable delivery system," *Adv. Mater.*, vol. 24, no. 20, pp. 2703–2709, 2012.

[36] J. Lopes, G. Santos, P. Barata, R. Oliveira, and C. Lopes, "Physical and Chemical Stimuli-Responsive Drug Delivery Systems: Targeted Delivery and Main Routes of Administration," *Curr. Pharm. Des.*, vol. 19, no. 41, pp. 7169–7184, Dec. 2013.

[37] A. C. H. Pape, M. H. Bakker, C. C. S. Tseng, M. M. C. Bastings, S. Koudstaal, P. Agostoni, S. A. J. Chamuleau, and P. Y. W. Dankers, "An Injectable and Drug-loaded Supramolecular Hydrogel for Local Catheter Injection into the Pig Heart," *J. Vis. Exp.*, no. 100, pp. 1–8, 2015.

[38] M. H. Bakker, R. E. Kieltyka, L. Albertazzi, and P. Y. W. Dankers, "Modular supramolecular ureidopyrimidinone polymer carriers for intracellular delivery," *RSC Adv.*, vol. 6, no. 112, pp.

110600–110603, 2016.

[39] S. Dennler, S. Itoh, D. Vivien, P. Ten Dijke, S. Phane Huet, and J.-M. Gauthier, “Direct binding of Smad3 and Smad4 to critical TGFβ-inducible elements in the promoter of human plasminogen activator inhibitor-type 1 gene,” *EMBO J.*, vol. 17, no. 11, pp. 3091–3100, 1998.

[40] G. J. Inman, F. J. Nicolás, J. F. Callahan, J. D. Harling, L. M. Gaster, A. D. Reith, N. J. Laping, and C. S. Hill, “SB-431542 is a potent and specific inhibitor of transforming growth factor-beta superfamily type I activin receptor-like kinase (ALK) receptors ALK4, ALK5, and ALK7.,” *Mol. Pharmacol.*, vol. 62, no. 1, pp. 65–74, Jul. 2002.

[41] N. J. Laping, E. Grygielko, A. Mathur, S. Butter, J. Bomberger, C. Tweed, W. Martin, J. Fornwald, R. Lehr, J. Harling, L. Gaster, J. F. Callahan, and B. A. Olson, “Inhibition of Transforming Growth Factor (TGF)-beta 1-Induced Extracellular Matrix with a Novel Inhibitor of the TGF-beta Type I Receptor Kinase Activity: SB-431542,” *Mol. Pharmacol.*, vol. 62, no. 1, pp. 58–64, Jul. 2002.

[42] S. K. Halder, R. D. Beauchamp, and P. K. Datta, “A Specific Inhibitor of TGF-β Receptor Kinase, SB-431542, as a Potent Antitumor Agent for Human Cancers,” *Neoplasia*, vol. 7, no. 5, pp. 509–521, 2005.

[43] M. Goebel-Stengel, A. Stengel, Y. Taché, and J. R. Reeve, “The importance of using the optimal plastic and glassware in studies involving peptides,” *Anal Biochem*, vol. 414, no. 1, pp. 38–46, 2011.

[44] R. W. Korsmeyer, R. Gurny, E. Doelker, P. Buri, and N. A. Peppas, “Mechanisms of solute release from porous hydrophilic polymers,” *Int. J. Pharm.*, vol. 15, no. 1, pp. 25–35, May 1983.

[45] N. A. Peppas and J. J. Sahlin, “A simple equation for the description of solute release. III. Coupling of diffusion and relaxation,” *Int. J. Pharm.*, vol. 57, no. 2, pp. 169–172, 1989.

[46] N. Andreu, A. Zelmer, and S. Wiles, “Noninvasive biophotonic imaging for studies of infectious disease,” *FEMS Microbiology Reviews*, vol. 35, no. 2. pp. 360–394, 2011.

[47] S. I. S. Hendrikse, S. Spaans, E. W. Meijer, and P. Y. W. Dankers, “Supramolecular Platform Stabilizing Growth Factors,” *Biomacromolecules*, vol. 19, no. 7, pp. 2610–2617, 2018.

[48] T. Mahmood and P. C. Yang, “Western blot: Technique, theory, and trouble shooting,” *N. Am. J. Med. Sci.*, vol. 4, no. 9, pp. 429–434, 2012.

[49] J. Zhu, F. He, S. Hu, and J. Yu, “On the nature of human housekeeping genes,” *Trends Genet.*, vol. 24, no. 10, pp. 481–484, Oct. 2008.

[50] K. J. Livak and T. D. Schmittgen, “Analysis of relative gene expression data using real-time quantitative PCR and the 2-ΔΔCT method,” *Methods*, vol. 25, no. 4, pp. 402–408, 2001.

[51] M. Bujak and N. G. Frangogiannis, “The role of TGF-β signaling in myocardial infarction and cardiac remodeling,” *Cardiovascular Research*, vol. 74, no. 2. pp. 184–195, 2007.

[52] M. J. Webber, E. A. Appel, E. W. Meijer, and R. Langer, “Supramolecular biomaterials,” *Nature Materials*, vol. 15, no. 1. pp. 13–26, 2015.

[53] J. C. . Bischof and X. He, “Thermal Stability of Proteins,” *Ann. N. Y. Acad. Sci.*, vol. 1066, no. 1, pp. 12–33, Dec. 2005.

[54] M. H. Bakker, M. Grillaud, D. J. Wu, P.-P. P. K. H. H. Fransen, I. H. de Hingh, and P. Y. W. W. Dankers, “Cholesterol Modification of an Anticancer Drug for Efficient Incorporation into a Supramolecular Hydrogel System,” *Macromol. Rapid Commun.*, vol. 1800007, no. 17, pp. 1–6,

Sep. 2018.

[55] C. C. S. Tseng, S. Wenker, M. H. Bakker, A. O. Kraaijeveld, P. Y. W. Dankers, P. R. Seevinck, J. Smink, S. Kimmel, F. J. van Slochteren, and S. A. J. Chamuleau, "Active tracked intramyocardial catheter injections for regenerative therapy with real-time MR guidance : feasibility in the porcine heart," *Eurointervention*, 2018.

[56] P. Y. W. Dankers, M. J. A. Van Luyn, A. Huizinga-Van Der Vlag, A. H. Petersen, J. A. Koerts, A. W. Bosman, and E. R. Popa, "Convenient formulation and application of a supramolecular ureido-pyrimidinone modified poly(ethylene glycol) carrier for intrarenal growth factor delivery," *Eur. Polym. J.*, vol. 72, pp. 484–493, Nov. 2015.

[57] N. A. Peppas, P. Bures, W. Leobandung, and H. Ichikawa, "Hydrogels in pharmaceutical formulations," *Eur. J. Pharm. Biopharm.*, vol. 50, pp. 27–46, 2000.

[58] T. Tanaka, "Phase transitions in gels and a single polymer," *Polymer (Guildf).*, vol. 20, no. 11, pp. 1404–1412, 1979.

[59] N. Peppas, "Physiologically responsive gels," *J. Bioact. Compat. Polym.*, vol. 6, pp. 241–246, 1991.

[60] E. Holowka and S. Bhatia, "Controlled-Release Systems," in *Drug Delilvery: Materials Design and Clinical Perspective*, New York: Springer, New York, NY, 2014, pp. 7–62.

[61] J. Siepmann and N. A. Peppas, "Modeling of drug release from delivery systems based on hydroxypropyl methylcellulose (HPMC)," *Advanced Drug Delivery Reviews*, vol. 64. pp. 163–174, 2012.

[62] M. Maeda, K. R. Johnson, and M. J. Wheelock, "Cadherin switching: essential for behavioral but not morphological changes during an epithelium-to-mesenchyme transition," *J. Cell Sci.*, vol. 118, no. 5, pp. 873–887, Mar. 2005.

[63] M. A. Cichon, C. M. Nelson, and D. C. Radisky, "Regulation of epithelial-mesenchymal transition in breast cancer cells by cell contact and adhesion," *Cancer Inform.*, vol. 14, pp. 1–13, Feb. 2015.

[64] E. Batlle, E. Sancho, C. Francí, D. Domínguez, M. Monfar, J. Baulida, and A. G. De Herreros, "The transcription factor Snail is a repressor of E-cadherin gene expression in epithelial tumour cells," *Nat. Cell Biol.*, vol. 2, no. February, pp. 84–89, 2000.

[65] A. Cano, M. A. Pérez-Moreno, I. Rodrigo, A. Locascio, M. J. Blanco, M. G. Del Barrio, F. Portillo, and M. A. Nieto, "The transcription factor Snail controls epithelial-mesenchymal transitions by repressing E-cadherin expression," *Nat. Cell Biol.*, vol. 2, no. 2, pp. 76–83, 2000.

[66] H. Yu, Y. Shen, J. Hong, Q. Xia, F. Zhou, and X. Liu, "The contribution of TGF-β in epithelial–mesenchymal transition (EMT): Down-regulation of E-cadherin via snail," *Neoplasma*, vol. 62, no. 1. pp. 1–15, 2015.